

Calix[n]arene-Based Glycoclusters: Bioactivity of Thiourea-Linked Galactose/Lactose Moieties as Inhibitors of Binding of Medically Relevant Lectins to a Glycoprotein and Cell-Surface Glycoconjugates and Selectivity among Human Adhesion/Growth-Regulatory Galectins

Sabine André,^[a] Francesco Sansone,^[b] Herbert Kaltner,^[a] Alessandro Casnati,^[b] Jürgen Kopitz,^[c] Hans-Joachim Gabius,*^[a] and Rocco Ungaro*^[b]

*Growing insights into the functionality of lectin–carbohydrate interactions are identifying attractive new targets for drug design. As glycan recognition is regulated by the structure of the sugar epitope and also by topological aspects of its presentation, a suitable arrangement of ligands in synthetic glycoclusters has the potential to enhance their avidity and selectivity. If adequately realized, such compounds might find medical applications. This is why we focused on lectins of clinical interest, acting either as a potent biohazard (a toxin from *Viscum album* L. akin to ricin) or as a factor in tumor progression (human galectins-1, -3, and -4). Using a set of 14 calix[n]arenes (n=4, 6, and 8) with thiourea-linked galactose or lactose moieties, we first ascertained the lectin-binding properties of the derivatized sugar head groups conjugated to the synthetic macrocycles. Despite their high*

degree of flexibility, the calix[6,8]arenes proved especially effective for the plant AB-toxin, in the solid-phase model system with a single glycoprotein (asialofetuin) and with human tumor cells in vitro. The bioactivity of the calix[n]arenes was also proven for human galectins. Notably, selectivity for the tested tandem-repeat-type galectin-4 among the three subgroups was determined at the level of solid-phase and cell assays, the large flexible macrocycles again figuring prominently as inhibitors. Alternate and cone versions of calix[4]arene with lactose units distinguished between galectins-1 and -4 versus galectin-3 in cell assays. The results thus revealed bioactivity of galactose-/lactose-presenting calix[n]arenes for medically relevant lectins and selectivity within the family of adhesion/growth-regulatory human galectins.

Introduction

Cell-surface glycans are far more than a means of protecting proteins from proteolysis or affecting charge density. In fact, cells derive a significant portion of their ability for intercellular communication from glycan structures. They equal peptide sequences of proteins in being biochemical signals.^[1] Processing of the sugar-encoded messages and their translation into cellular responses involves carbohydrate-binding proteins (lectins).^[2] This discovery of functional lectin–carbohydrate interactions signifies a new route for drug design. Firstly, suitable targets need to be identified. Unquestionably, protection against biohazardous plant toxins and the interference in lectin-mediated processes during tumor progression are aims warranting serious efforts.


Medically oriented reasoning has directed our attention to galactoside-binding AB toxins such as ricin or the *Viscum album* agglutinin (VAA) and the galectin family of endogenous lectins. Among its three subgroups, that is, homodimeric proto-type, chimera-type, and tandem-repeat-type proteins, immunohistochemical fingerprinting had revealed an unfavorable relationship of galectin expression to prognosis in several tumor systems, for example in colon cancer for galectin-1 (proto-type), galectin-3 (chimera-type), and galectin-4 (tandem-repeat-type).^[3] Capitalizing on convenient access to human lec-

tins by recombinant production, their reactivity with test compounds can be readily profiled as is routinely done for plant lectins. In doing so, the sensitivity of galectin binding to the local density of cognate determinants in *N*- and *O*-glycans and glycodendrimers had been documented, as was also ascertained for the plant toxin.^[4] These results encouraged us to design glycoclusters with variations in ligand density and in presentation, and then to assess their inhibitory potencies to identify potent candidates for further refinement. Conjugation

[a] Priv. Doz. Dr. S. André, Prof. Dr. H. Kaltner, Prof. Dr. H.-J. Gabius
Institut für Physiologische Chemie, Tierärztliche Fakultät
Ludwig-Maximilians-Universität
Veterinärstrasse 13, 80539 München (Germany)
E-mail: gabius@lectins.de

[b] Dr. F. Sansone, Prof. Dr. A. Casnati, Prof. Dr. R. Ungaro
Dipartimento di Chimica Organica e Industriale, Università degli Studi
V. le G. P. Usberti 17A, 43100 Parma (Italy)
E-mail: ungaro@unipr.it

[c] Prof. Dr. J. Kopitz
Institut für Angewandte Tumorbologie, Zentrum Pathologie,
Klinikum der Ruprecht-Karls-Universität Heidelberg
Im Neuenheimer Feld 220, 69120 Heidelberg (Germany)

 Supporting information for this article is available on the WWW under <http://www.chembiochem.org> or from the author.

of sugar moieties to a macrocycle is a reasonable step in this research program. In this report, we addressed this synthetic challenge and merged preparative work with biochemical and cell biological assays.

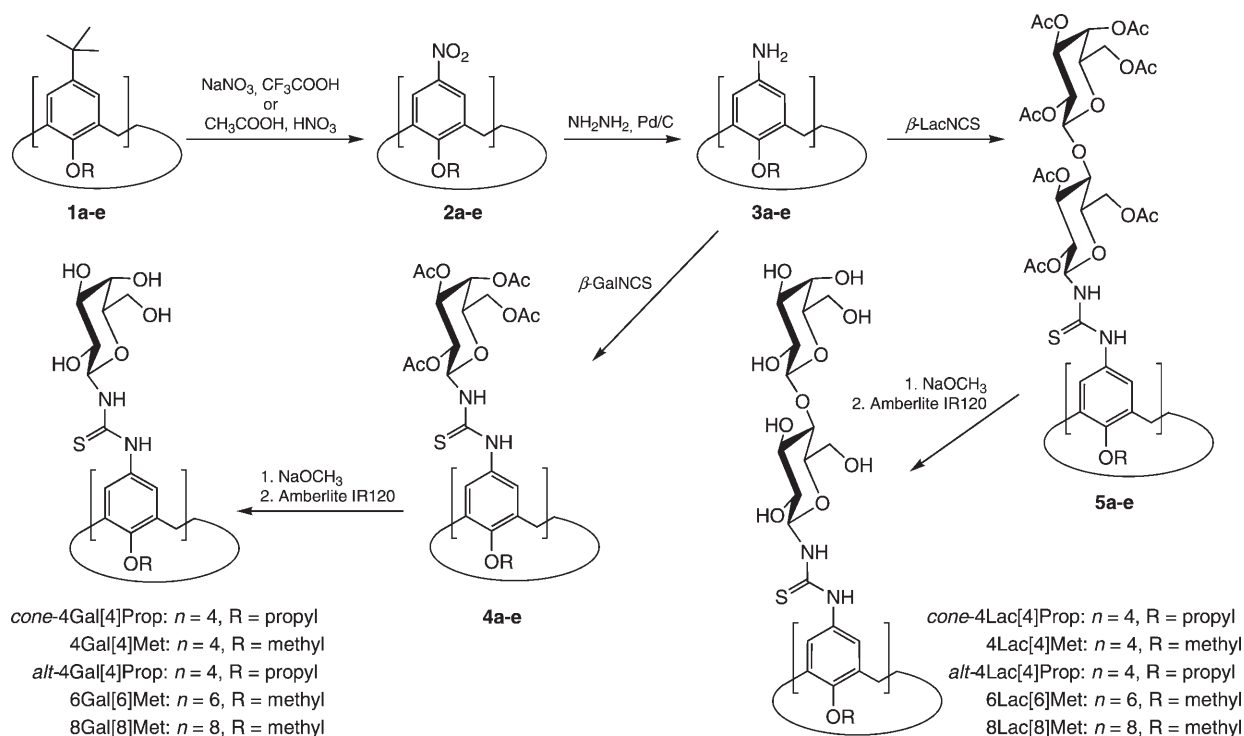
A cyclic platform for introducing lectin ligands offers the advantage of a certain degree of backbone rigidity. As examples, fused six-membered imide ring systems, cyclic decapeptides, cyclodextrins, cyclophanes, and phenol-formaldehyde cyclic oligomers (calixarenes) have been demonstrated to undergo facile synthetic incorporation of carbohydrate moieties.^[5] Herein, we focus on calix[*n*]arenes, covalently adding substituted galactose or lactose moieties to the scaffold. Compared to other macrocyclic compounds calix[*n*]arenes offer the unique opportunity for introducing variations of ring size, molecular shape, conformational flexibility, symmetry, and valency. The option for a thiourea linker was chosen to enable an easy amine/isothiocyanate reaction and to allow potential hydrogen bonding.^[6] Following the synthesis of the panel of 14 glycoclusters with two to eight sugar moieties per macrocycle and their chemical characterization, we revealed lectin-binding properties in a solid-phase assay using a potent plant toxin (VAA) and the three mentioned human galectins. With the lectin-binding property of the glycoclusters documented, inhibitory capacity was comparatively assessed in each case. On the grounds that medical application is envisioned we proceeded to test the glycoclusters as inhibitors of lectin binding to human tumor cells in vitro. The glycomic complexity of cell surfaces in terms of structural diversity and dynamic changes in local epitope density can have a profound effect on lectin-binding properties not mimicked in solid-phase assays (for details, see ref. [1]). The following questions will be answered by

the combined set of experiments: will the substituted sugar moieties maintain ligand activity? Will glycocluster design enhance avidity relative to free sugar? Will there be selectivity between lectin type and glycocluster design?

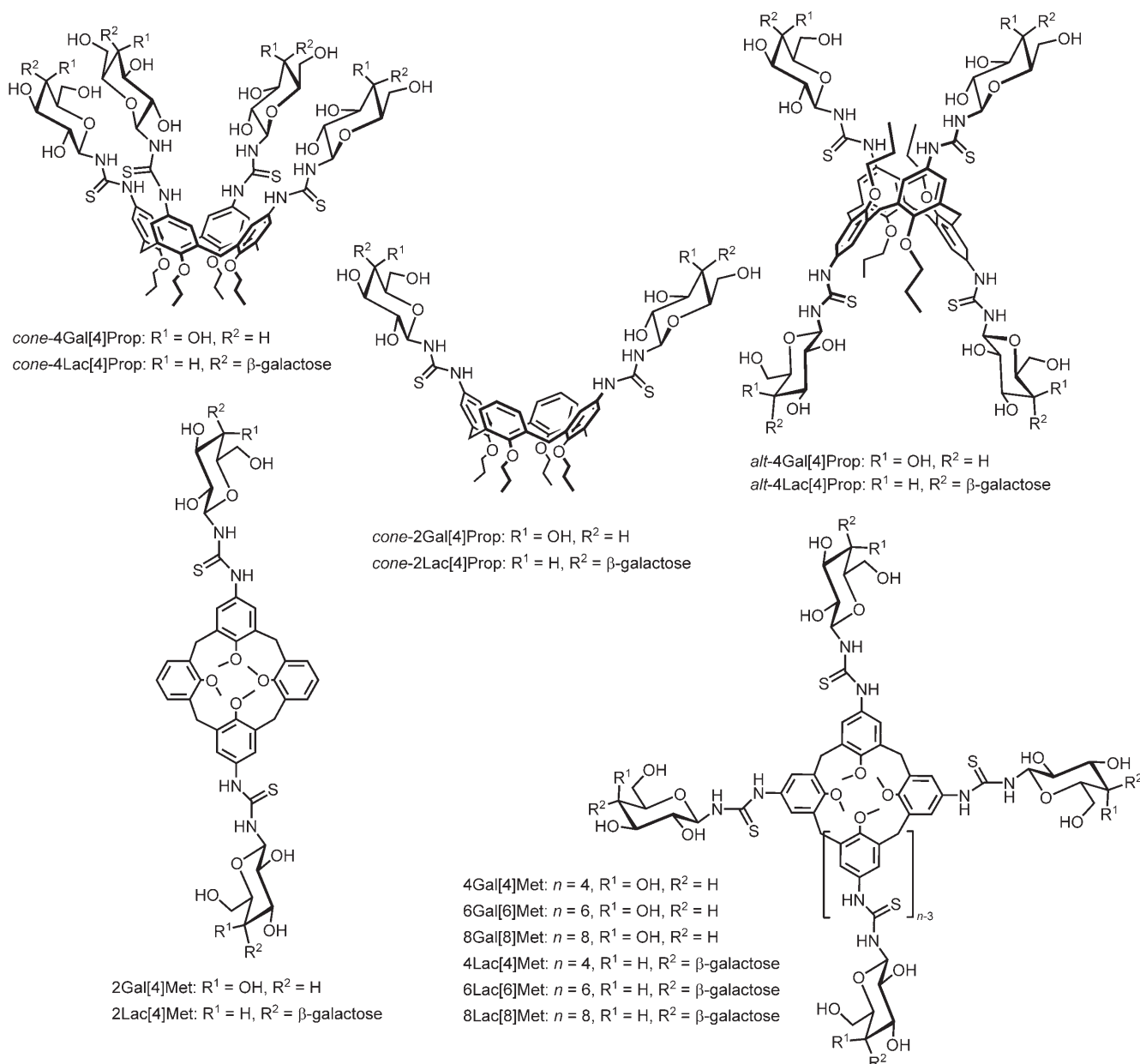
Results

Synthesis and conformational properties of calix[*n*]arene glycoclusters

Functionalization of the alkoxy-calix[*n*]arenes to obtain fully glycosylated compounds was performed at the upper rim (aromatic nuclei) in four steps (Scheme 1) through ipso nitration (aromatic nucle) in four steps (Scheme 1) through ipso nitration of the proper alkylated *p*-*tert*-butyl calixarenes to give **2a–e**, reduction to amines **3a–e** with hydrazine hydrate in the presence of Pd/C, condensation with β -galactosyl or β -lactosyl isothiocyanates to **4a–e** and **5a–e**, respectively, and, finally, deprotection from acetyl groups by the Zemplen method. Sugar condensation and deprotection were analogously performed to obtain the divalent ligands 2Gal[4]Met (for the meaning of this nomenclature see ref. [7]) and 2Lac[4]Met from the corresponding diamino derivatives. The thiourea linker structure was kept constant. The resulting glycoclusters cover different ways of sugar presentation, as shown. In detail, the compounds *cone*-4Gal[4]Prop,^[8] *cone*-4Lac[4]Prop, *cone*-2Gal[4]Prop,^[8] and *cone*-2Lac[4]Prop^[8] form the fixed-cone type, compounds *alt*-4Gal[4]Prop and *alt*-4Lac[4]Prop the 1,3-alternate type. If the substituent at the lower rim (phenolic oxygen atoms) is a methyl group, then dynamic flexibility ensues, applicable for compounds 4Gal[4]Met, 4Lac[4]Met, 2Gal[4]Met, and 2Lac[4]Met. The divalent derivatives show in CD₃OD the



Scheme 1. Synthesis of the fully glycosylated upper rim calix[*n*]arenes.



presence of conformers in slow exchange on the NMR time-scale. The two signals in ^{13}C NMR spectra at approximately 31 and 37 ppm, attributable to the bridging methylene groups^[9] (ArCH_2Ar), indicate that the cone and the 1,3-alternate are the most abundant conformations in solution. Detailed inspection of NMR spectra in D_2O for compounds 4Gal[4]Met and 4Lac[4]Met (see Table 1) revealed a 1,3-alternate conformation, especially by presenting in ^{13}C NMR spectra the diagnostic peak at 36.8 ppm (for 4Gal[4]Met) and 36.9 ppm (for 4Lac[4]Met; Table 1). The occurrence of sharp signals is an indication for monomer status in solution. In contrast, the NMR spectra of the calix[4]arenes *cone-4Gal[4]Prop* and *cone-4Lac[4]Prop*, poorly soluble in water, are comparatively broad in D_2O even when increasing the temperature to 363 K, pointing to a tendency for aggregation of these amphiphilic substances. Using deuterated methanol the cone structure was verified by identifying the two diagnostic doublets ($J_{\text{ab}} = 13.2$)

for the protons of the methylene bridge and the respective resonances at 31–32 ppm (Table 1) for the corresponding C atom. Regarding the tetrafunctionalized glycoconjugates, the fixed 1,3-alternate conformation of *alt-4Gal[4]Prop* and *alt-4Lac[4]Prop* was ascertained by picking up the typical singlet for methylene-bridge protons in HSQC experiments. Signals were sharp, excluding major tendency for aggregation.

In comparison to these compounds, the glycoconjugates originating from calix[6]- (6Gal[6]Met, 6Lac[6]Met) and calix[8]arenes (8Gal[8]Met, 8Lac[8]Met) have enhanced flexibility. Increase in ring size and the presence of the small methoxy substituent at the lower rim are factors favoring this inherently large degree of dynamics. In addition to drawing on the available structural data of calix[6]- or calix[8]arenes,^[10] we performed molecular modeling on compound 8Lac[8]Met using the classical molecular mechanics force field (MMFF), which resulted in two energetically minimized conformations referred

Table 1. Analytical data of the calix[n]arene-based glycoclusters.

| Compound | H1 and H1' | δ | | CS | C1 and C1' | ESI-MS [M+Na] ⁺ (calcd)/ *[M+2Na] ²⁺ (calcd) |
|---|---|---|---|------------------------|--|--|
| | | ¹ H | ArCH ₂ Ar ¹³ C | | | |
| <i>cone</i> -4Gal[4]Prop ^[a] | 5.51 | 4.51, 3.21 | 32.3 | 183.2 | 86.4 | 1559.4 (1559.5) |
| 4Gal[4]Met | 5.42 | 3.75 ^[c] | 36.8 | 183.6 | 86.1 | 1447.8 (1447.4) *735.8 (735.2) |
| <i>alt</i> -4Gal[4]Prop | 5.44 | 3.81 ^[c] | 38.2 | 184.7 | 86.7 | 1559.5 (1559.5) |
| 6Gal[6]Met | 5.29 ^[d] | 3.92 ^[c,d] | 30.9 ^[b] | 182.3 ^[b] | 83.5 ^[b] | 2160.0 (2159.6) *1091.5 (1091.3) |
| 8Gal[8]Met | 5.23 ^[d] | 3.84 ^[c,d] | 30.1 ^[b] | 182.7 ^[b] | 84.7 ^[b] | *1447.2 (1447.4) |
| <i>cone</i> -4Lac[4]Prop | 5.40 ^[d] and 4.40 ^[d] | 4.23 ^[d] , 3.10 ^[d] | 30.9 ^[b] | 182.4 ^[b] | 83.9 ^[b] and 104.1 ^[b] | 2207.8 (2207.7) *1115.5 (1115.4) |
| 4Lac[4]Met | 5.47 and 4.42 | 3.73 ^[c] | 36.9 | 183.5 | 85.4 and 104.4 | 2096.7 (2095.6) 1059.7 (1059.3) |
| <i>alt</i> -4Lac[4]Prop | 5.49 and 4.50 | 3.72 ^[c] | 38.0 | 183.6 | 85.4 and 104.6 | 2207.6 (2207.7) *1115.3 (1115.4) |
| 6Lac[6]Met | 5.18 ^[d,e] and 4.18 ^[d,e] | 3.71 ^[c,d,e] | 30.8 ^[d,e] | 183.1 ^[d,e] | 84.4 ^[d,e] and 103.5 ^[d,e] | *1577.4 (1577.5) |
| 8Lac[8]Met | 5.24 ^[d] and 4.27 ^[d] | 3.75 ^[c,d] | 30.1 ^[d] | 184.1 ^[d] | 82.7 ^[d] and 102.2 ^[d] | *2095.3 (2095.6) |

[a] Taken from ref. [8] (CD₃OD). [b] [D₆]DMSO. [c] Value determined by correlation with the corresponding signal of the ArCH₂Ar carbon in the HSQC experiment. [d] Determined at 363 K. [e] D₂O + 5% [D₆]DMSO.

to as double-partial cone (Figure 1A) and 1,2-alternate (see Figure S1A in the Supporting Information) according to the literature.^[10] As a result of the occurrence of the pleated-loop conformer of octahydroxy-*p*-*tert*-butylcalix[8]arene in the solid state, we also calculated the energy of this structure (Figure 1B) to be 1206 kcal mol⁻¹, rather similar to the values found for the 1,2-alternate (1169 kcal mol⁻¹) and double-partial cone (1191 kcal mol⁻¹) structures. Having prepared the panel of glycoclusters and examined their conformational properties, the next step was to test the compounds to determine whether the calix[n]arene-presented galactose/lactose moieties have ligand properties with medical perspective.

Solid-phase inhibition assays

The lectin–ligand interaction system consisted of a microtiter plate surface, to which the glycoprotein asialofetuin (ASF) was adsorbed, and the labeled lectin in solution. The coating densi-

ty and the lectin concentration needed to be adjusted to yield a signal intensity in the linear range to avoid complications resulting from working at plateau levels. This initial protocol was completed for the toxic plant lectin and the human galectins. It included controls with haptenic inhibitors and ascertaining carbohydrate-dependent binding of the lectins to the matrix in each case. Having set up a valid test system, free mono- and disaccharides and then the panel of the 14 glycoclusters could systematically be studied. As illustrated with representative examples in Figure 2 for galactose and Figure 3 for lactose, substantial inhibition was obtained with the free mono- and disaccharides. As a result of solubility problems for certain calix[n]arenes (see above) stock solutions were prepared in dimethyl sulfoxide and then diluted in buffer prior to use. Up to 4.4% aprotic solvent (at 2.5 mM lactose content) was then present in the assay, therefore the corresponding control values were routinely determined under identical conditions and in the absence of solvent to spot any effect of solvent presence. Thus

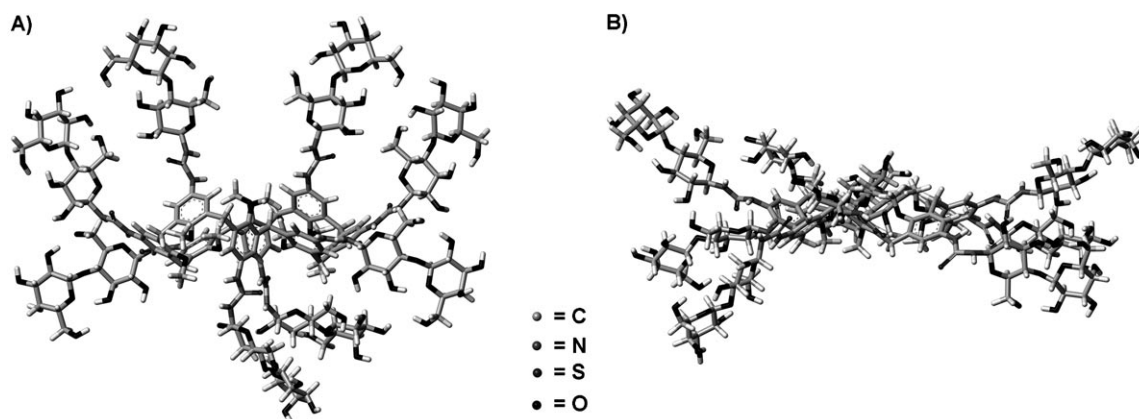


Figure 1. Lateral view of the minimized A) double-partial cone and B) pleated-loop conformation of octalactosylthioureidocalix[8]arene (8Lac[8]Met). For different views and color pictures see Figures S1 and S2 in the Supporting Information.

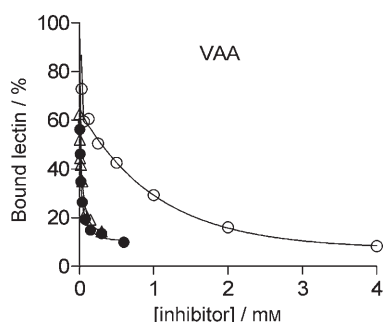


Figure 2. Inhibition by calix[n]arene-based glycoclusters carrying galactose (Δ : 8Gal[8]Met, \bullet : 6Gal[6]Met) of the binding of biotinylated VAA to surface-immobilized asialofetuin. Galactose (\circ) was used as control (please see Table 2 for IC_{50} values). The concentration of inhibitor is given with respect to galactose in all cases.

| Type of inhibitor | Gal units per molecule | IC_{50} [μ M] ^[b] |
|--------------------------|------------------------|-------------------------------------|
| <i>cone</i> -2Gal[4]Prop | 2 | 5000 |
| <i>cone</i> -4Gal[4]Prop | 4 | 300 |
| 2Gal[4]Met | 2 | 2000 |
| 4Gal[4]Met | 4 | 2500 |
| <i>alt</i> -4Gal[4]Prop | 4 | 2000 |
| 6Gal[6]Met | 6 | 5 |
| 8Gal[8]Met | 8 | 8 |
| galactose | 1 | 600 |

[a] Amount of ASF for coating: 0.25 μ g; lectin concentration: 0.5 μ g mL⁻¹.
[b] IC_{50} values in μ M sugar per assay.

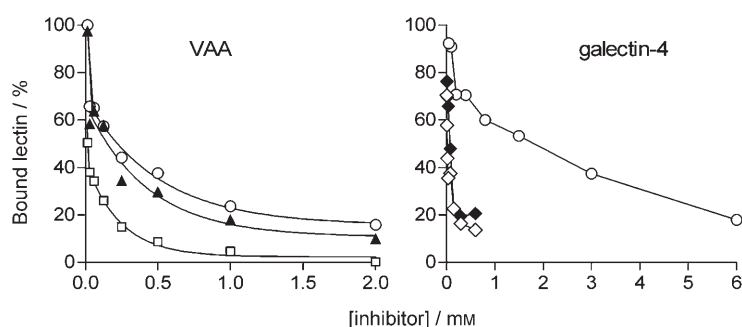


Figure 3. Inhibition by calix[n]arene-based glycoclusters carrying lactose of the binding of biotinylated VAA (left) and human galectin-4 (right) to surface-immobilized asialofetuin. Lactose (\circ) was used as control (see Table 3 for IC_{50} values). Data on the following compounds are presented: 8Lac[8]Met (\square) and *alt*-4Lac[4]Prop (\blacktriangle) in the case of VAA, *cone*-4Lac[4]Prop (\circ), and 4Lac[4]Met (\blacklozenge) in the case of galectin-4. The concentration of inhibitor is given with respect to lactose in all cases.

the test system is suitable to answer the question whether the sugar moieties in the calix[n]arenes are capable of acting as lectin inhibitors.

The glycoclusters were added to the lectin-containing solution in successively decreasing concentrations, and the ensuing effect on the extent of lectin binding is shown in Figure 2 and Figure 3 and summarized for all tested compounds in Tables 2 and 3. To allow direct comparison between free sugar and glycoclusters, the concentration of the test compound is expressed in μ M sugar added to the assay. Evidently, the conjugated sugars maintained their inhibitory activity. Topological parameters made their mark on the sugars' potency in this respect. Clustering on macrocycles was especially effective for the plant toxin and galectin-4 (Figure 3, Table 3). Among the human lectins, different response patterns were registered, the tandem-repeat-type galectin-4 reacted very sensitive-

ly to the presence of these test compounds. The IC_{50} value for lactose was lowered by a factor of up to 300-fold relative to free sugar, when calculating the sugar concentration in the assay. This activity profile was retained after deletion of the linker region by genetic engineering, which turned galectin-4 into a prototype-like protein with two different carbohydrate recognition domains. Further testing of the N-terminal domain of this lectin also proved the efficacy of the glycoclusters in this system, implying that the structural features of this lectin site make a sizeable contribution. Relative to galectins-1 and -3, properties of the substituted lactose appeared to contribute to the potency toward galectin-4.

Using this test system with a single type of glycoprotein with three complex-type N-glycans, mostly triantennary, and three core 1 disaccharides, inhibitory activity was determined by discerning different degrees of enhancement relative to the free sugar and a preference for the tandem-repeat-type galectin-4. Compared to this model, cell surfaces present a wide array of glycan chains with diverse lectin-reactive determinants undergoing dynamic lateral movements. Also, spatial parameters governing accessibility may come into play. Envisioning medical applications it thus is essential to determine the activity of glycoclusters in cell-binding assays.

| Type of inhibitor | Lac units per molecule | VAA [0.5 μ g mL ⁻¹] | Galectin-1 [10 μ g mL ⁻¹] | Galectin-3 [5 μ g mL ⁻¹] | Galectin-4 [5 μ g mL ⁻¹] |
|--------------------------|------------------------|-------------------------------------|---|--|--|
| <i>cone</i> -2Lac[4]Prop | 2 | 1000 | n.i. ^[b] | 2000 | 5 |
| <i>cone</i> -4Lac[4]Prop | 4 | 125 | 10000 | 200 | 20 |
| 2Lac[4]Met | 2 | 800 | n.i. ^[b] | 2500 | 1000 |
| 4Lac[4]Met | 4 | 125 | 2000 | 600 | 40 |
| <i>alt</i> -4Lac[4]Prop | 4 | 200 | 1250 | 500 | 80 |
| 6Lac[6]Met | 6 | 15 | 600 | 400 | 5 |
| 8Lac[8]Met | 8 | 15 | 1250 | 300 | 40 |
| Lactose | 1 | 300 | 7500 | 2500 | 1500 |

[a] Amount of ASF for coating: 0.5 μ g, IC_{50} values in μ M sugar per assay. [b] n.i. = not inhibitory at 10 mM.

Cell-binding inhibition assays

Established human tumor lines were selected for this part of the study. Their lectin-binding properties are stable features. Nonetheless, in order to avoid any variability due to changes in length of culture time during the passage or medium composition, comparative experiments were performed with aliquots of identical cell batches at the same time. The fluorescent staining due to binding of labeled lectins was routinely analyzed on 10 000 cells, Figures 4–7 show fluorescence intensity in relation to cell number. In each case, dependence of cell staining, measured in percentage of positive cells and mean channel fluorescence intensity (all numbers are given in Figures 4–7), from concentration of the labeled probe and concentration of free sugar was characterized, see the top panel of Figure 4 for an example. Selecting a distinct reference concentration of free sugar reaching partial inhibition, the relative effect of calix[*n*]arene presence on cell binding could be determined.

Glycoclusters with lactose or galactose head groups were active for the plant toxin at this level, too (Figure 4 and Figure S3 in the Supporting Information). As the monitoring of cell fluorescence revealed, the IC_{50} values in the solid-phase assay will not automatically translate into a direct ranking in the cell assays (Figure 4). The 2Lac[4]Met and cone-2Lac[4]Prop compounds showed a relatively increased potency, whereas the alt-4Lac[4]Prop compound remained rather similar to lactose in inhibitory efficacy and 6Lac[6]Met and 8Lac[8]Met are less active (Figure 4). Regarding the human lectins, in the case of galectin-1 cone-4Lac[4]Prop, a weak inhibitor surpassed by lactose on solid-phase assays, remained weak, whereas the compounds 6Lac[6]Met and especially 8Lac[8]Met and also 2Lac[4]Met, 4Lac[4]Met, and alt-4Lac[4]Prop proved effective (Figure 5). Glycosylated calix[*n*]arenes similarly interfered with binding of galectin-3 to human colon cancer cells (Figure 6). Cone-4Lac[4]Prop was the most favorable inhibitor in both assay types. Figure 6 presents the difference between lactose (A) and this compound (B) in keeping the lectin away from the cell surface. Evidently, this calix[4]arene will affect galectins-1 and -3 differently (Figures 5 and 6). Interestingly, it was also a rather weak inhibitor (for a calix[*n*]arene) of galectin-4 binding (Figure 7).

In stark contrast, the alt-4Lac[4]Prop conformer was conspicuously more active than the cone-type glycocluster for galectin-1, a property shared by galectin-4 (Figures 5 and 7). In numbers (Figure 7), with the latter galectin, free lactose was rather ineffective up to 10 mM (50% positive cells, 25.6 as mean fluorescence intensity), the divalent cone version at 1 μ M lactose led to decreases to 38.1%/17.4. Even at the considerably lowered concentration of 0.2 μ M, the corresponding tetravalent alt-cluster fared much better as an inhibitor with data of 20.4%/9.2 (for information on galectin-1, please see numbers in Figure 5). As a means to interfere with binding of galectins-1 and -4 in a coordinated manner this glycocluster is a viable option. Altogether, the bioactivity of the calix[*n*]arenes on galectin-4 binding is especially noteworthy, because free lactose up to 10 mM was a comparatively weak inhibitor of cell bind-

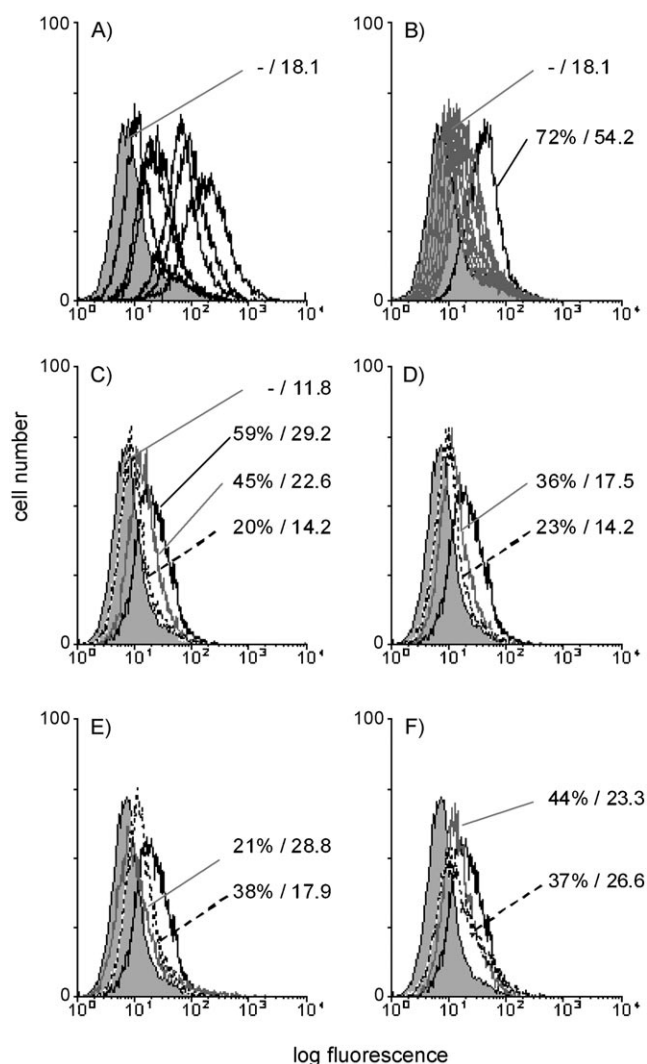


Figure 4. Semilogarithmic representation of the fluorescent surface staining of cells of the human B-lymphoblastoid line Croco II by labeled VAA. The control value representing staining by second-step reagent in the absence of lectin is given as shaded area. Concentration dependence for the probe was tested at 0.05, 0.1, 0.2, 0.5, 1, and 2 μ g mL⁻¹ (A) and the extent of inhibition by lactose was determined at the constant lectin concentration of 0.2 μ g mL⁻¹ using sugar (lactose) concentrations of 0.5, 1, 2, 4, 8, 10, 20, and 50 mM (B). Control data are inserted for lectin-independent staining (A, B, C) and staining at 0.2 μ g mL⁻¹ lectin (B). Lactose and calix[*n*]arene-based glycoclusters as inhibitors of lectin binding at 0.2 μ g mL⁻¹ were used at the sugar concentration of 2 mM, shown in the following order: C) lactose (gray line) and 2Lac[4]Met (dashed line); D) 8Lac[8]Met (gray line) and cone-4Lac[4]Prop (dashed line); E) cone-2Lac[4]Prop (gray line) and 4Lac[4]Met (dashed line); F) alt-4Lac[4]Prop (gray line) and 6Lac[6]Met (dashed line). The black line in C–F represents the control value of lectin-dependent staining in the absence of inhibitor. Quantitative data on the percentage of positive cells and mean channel fluorescence are given in each panel.

ing (Figure 7). Blocking association of this human lectin to the cell surface will thus depend on an avidity increase by cluster design. In full accord with the data from the solid-phase assays, sugar conjugation had a large effect on inhibitory potency. Tested at 0.1 μ M the compound 6Lac[6]Met proved most effective (Figure 7). This substance further underscores the potential for differential reactivity in the galectin family, because

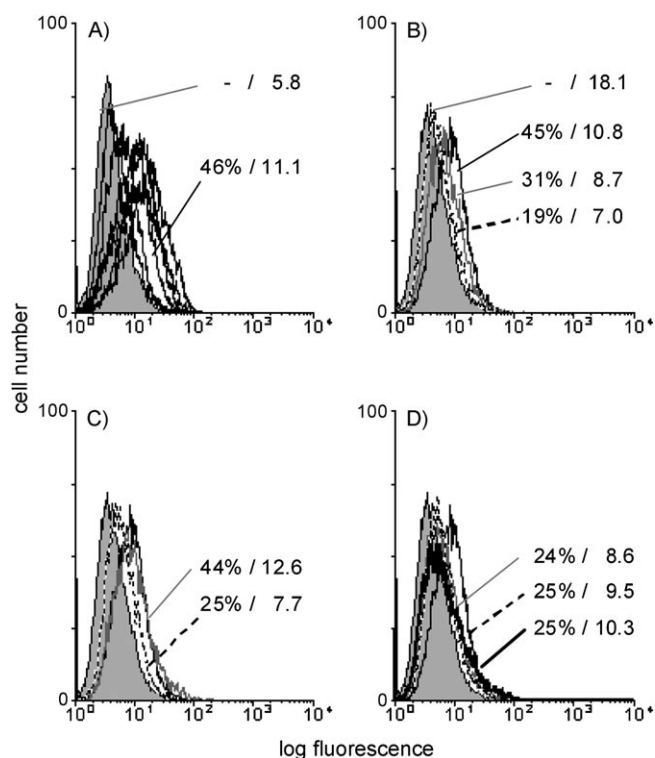


Figure 5. Semilogarithmic representation of the fluorescent surface staining of cells of the human pancreatic carcinoma line Capan-1, reconstituted for expression of the tumor suppressor p16^{INK4a}, by labeled galectin-1. The control value representing staining by second-step reagent in the absence of lectin is given as shaded area. Concentration dependence for the probe was tested at 2, 5, 10, 20, 30, and 40 $\mu\text{g mL}^{-1}$ (A). Control data are inserted for lectin-independent background and staining at 10 $\mu\text{g mL}^{-1}$ lectin. Using the constant lectin concentration at 10 $\mu\text{g mL}^{-1}$, lactose and calix[n]arene-based glycoclusters as inhibitors were used at the sugar concentration of 2 mM, shown in the following order: B) lactose (gray line) and 8Lac[8]Met (dashed line); C) cone-4Lac[4]Prop (gray line) and 4Lac[4]Met (dashed line); D) alt-4Lac[4]Prop (gray line), 2Lac[4]Met (dashed line), and 6Lac[6]Met (bold black line). Numbers characterizing cell reactivity are always given in the order of listing. The black line in the top right and in the bottom panels represents the control value of lectin-dependent staining in the absence of inhibitor. Quantitative data on the percentage of positive cells and mean channel fluorescence are given in each panel.

it showed preference to interfere with binding of galectins-1 and -4 versus galectin-3 (Figures 5–7).

Discussion

Multivalency of natural glycans is a key factor to produce the tangible benefits of high affinity and selectivity in lectin–carbohydrate interactions.^[1b–d,11] Intuitively, a matching design of sugar units in glycoclusters to target distinct lectins is a salient step toward development of potent inhibitors. That particular glycosignatures, for example, of yeast and bacteria that cause infections, are reliably identified by host defense lectins signifies the importance of ligand topology as a parameter to guide target selection.^[1d] The long-term aim to develop custom-made neoglycoconjugates ties synthetic work, here on calix[n]arenes as a platform for chemical glycosylation, to experiments which assess the actual glycocluster efficacy to

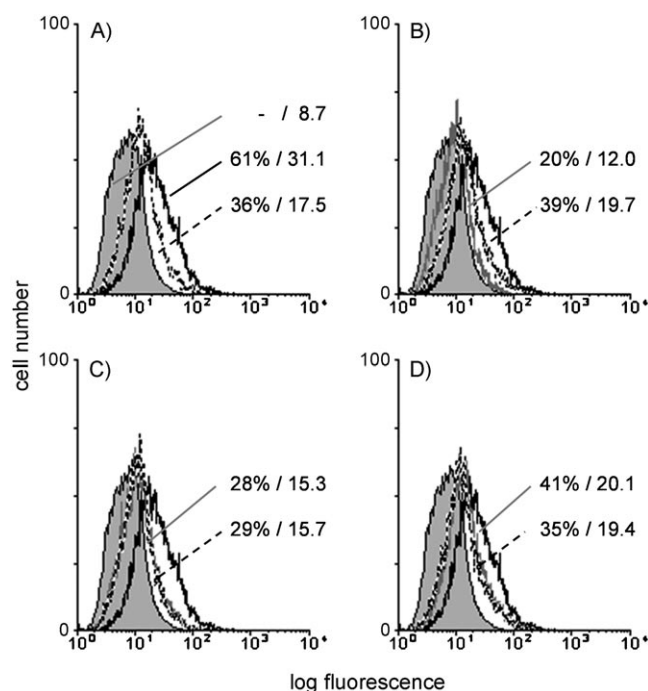


Figure 6. Semilogarithmic representation of the fluorescent surface staining of cells of the human colon adenocarcinoma cell line SW480 by labeled galectin-3. The control value representing staining by second-step reagent in the absence of lectin is given as shaded area. Using the constant lectin concentration at 10 $\mu\text{g mL}^{-1}$, control values in the absence of lectin (shaded area) and in the absence of inhibitor (A, black line) calibrate the inhibitory potential of lactose (top panel, left: dashed line) and the following calix[n]arene-based glycoclusters at the sugar concentration of 0.1 mM: B) cone-4Lac[4]Prop (gray line), 6Lac[6]Met (dashed line); C) 8Lac[8]Met (gray line) and 4Lac[4]Met (dashed line); D) alt-4Lac[4]Prop (gray line) and 2Lac[4]Met (dashed line). The black line in all panels represents the control value of lectin-dependent staining in the absence of inhibitor. Quantitative data on the percentage of positive cells and mean channel fluorescence are given in each panel.

block lectin binding. With a medical perspective in mind, we selected a plant toxin and three adhesion/growth-regulatory human lectins representing the different subgroups of the galectins. Equally important, we added work with tumor cells in vitro to running tests in the solid-phase system with a nonavalent glycoprotein (ASF) as ligand. In a stepwise manner, we answered the questions given in the introduction.

At the outset, all compounds were thoroughly characterized. Initial experiments demonstrated that the conjugation process did not impair the ligand's capacity to bind to the tested lectins. An increased efficiency of lactose derivatives relative to those of galactose was observed in the case of the plant toxin, here especially the fully accessible tyrosine-containing binding site in subdomain 2 γ of the lectin. This result is in full accord with previous inhibition and calorimetry studies, thus arguing in favor of compatibility of the linker with bioactivity.^[12] Normalizing all concentrations to the sugar, cluster effects were noted and quantified. Their occurrence applied both to binding to the model matrix and also to cell surfaces. Considering differences in presentation of lectin-binding sites between a model matrix and (real) cell surfaces, data obtained in solid-phase assays should be evaluated in relation to work on cells.

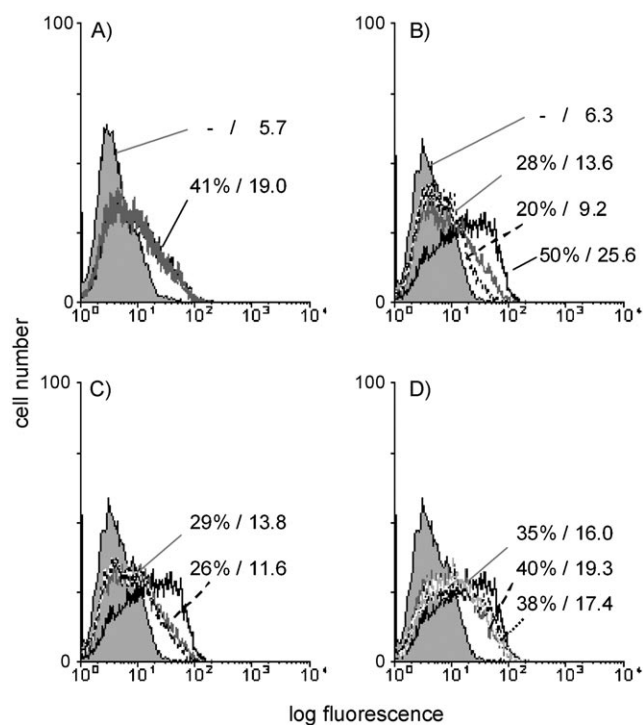


Figure 7. Semilogarithmic representation of the fluorescent surface staining of cells of the human pancreatic carcinoma line Capan-1, reconstituted for expression of the tumor suppressor p16^{INK4a}, by labeled galectin-4. The control value representing staining by second-step reagent in the absence of lectin is given as shaded area. The extent of inhibition by lactose was determined at the constant lectin concentration of 10 $\mu\text{g mL}^{-1}$ using sugar concentrations of 1, 2, 4, and 10 mM (A). Control data are inserted for lectin-independent staining and staining in the absence of inhibitor. Calix[n]arene-based glycoclusters as inhibitors (concentration of sugar given) are shown in the following order: B) 6Lac[6]Met (0.1 μM , gray line) and alt-4Lac[4]Prop (0.2 μM , dashed line); C) 8Lac[8]Met (0.2 μM , gray line) and 4Lac[4]Met (0.5 μM , dashed line); D) 2Lac[4]Met (0.5 μM , gray line), cone-2Lac[4]Prop (0.5 μM , dashed black line), and cone-4Lac[4]Prop (1 μM , dashed gray line). Numbers characterizing cell reactivity are always given in the order of listing. The black line in all panels represents the control value of lectin-dependent staining in the absence of inhibitor. Quantitative data on the percentage of positive cells and mean channel fluorescence are given in each panel.

Corroborating the given evidence for the plant toxin, ligand activity was also maintained for the tested galectins. The presentation of lactose on a cyclic platform with the given orientations slightly improves its inhibitory capacity for galectins-1 and -3, as previously seen for persubstituted β -cyclodextrins.^[13] Structurally, the chimera-type galectin-3 is unique in this lectin family. It is known to form pentamers when in contact with multivalent ligands, very favorably reacting with trivalent clusters established by coupling of prop-2-ynyl lactoside to a triiodobenzene core.^[14] The results presented here further elaborate the characteristics of sensitivity of galectins-1 and -3 toward shaping topology of the presented ligand.

What is apparent and novel are 1) the conspicuous effect of the calix[n]arenes on the tandem-repeat-type galectin-4 and 2) the possibility to combine effects on galectins-1 and -4 with one compound (a highly unfavorable expression signature for prognosis in colon cancer^[3d]). In the case of galectin-4, the relative inhibitory potency was markedly enhanced relative to free

lactose in both assay types. The respective IC₅₀ values revealed an obvious preference of this type of glycocluster for galectin-4, when compared to the two tested members of the other groups of galectins. The design of a deletion mutant for galectin-4 without the linker peptide was instrumental to intimate that presence of the linker was not an essential factor for this feature. Because the contributions of enthalpy and entropy to thermodynamics of binding N-acetyllactosamine differ between galectins-1, -3, and -4,^[15] it is likely that the interaction properties of the spacers to each lectin site may individually contribute to this attribute. Examining the known ligand profile of galectin-4 provides evidence for structural disparities in the binding site despite the shared affinity to lactose. Of note, galectin-4 strongly interacts with O-linked sulfoglycans, sulfatide with long-chain 2-hydroxylated fatty acids, and even cholesterol 3-sulfate, besides homing in on clustered T/T_n-antigens and ABH-blood group epitopes.^[4b,16] In clinical terms, expression of this lectin was linked to unfavorable prognosis in Dukes A and B colon tumors, related to malignant potential in hepatocellular carcinoma and to peritoneal metastasis of gastric cancer, found to be upregulated in mucinous epithelial ovarian cancer, and detected in breast cancer.^[3d,17] Within the physiological network of galectins in tumor cells,^[2b] galectin-4 may thus have discrete activity and expression patterns in certain tumor types, making it an attractive target of inhibitors in these instances. Further tailoring of the head group, for example by applying library approaches to galectins,^[18] might help increase the detected intrafamily selectivity, if the option for combined effects, as detected here, is not desirable. This work will likely also be required in order to distinguish this group member among the tandem-repeat-type galectins. Preliminary experiments on galectins-8 and -9 point to binding profiles which reflect structural similarity but can help identify nonuniform features.

In summary, we have prepared an array of calix[n]arenes presenting spacers galactose and lactose moieties and analyzed their reactivity towards a plant toxin and, for the first time, towards three human galectins. Inhibitory potency was determined in a solid-phase assay and a bioassay in vitro. Cluster effects were noted, particularly reactivity of glycoclusters registered for the tandem-repeat-type galectin-4. Its preferential reactivity to sulfoglycans gives ensuing work for head group tailoring a clear direction. Answering the final question posed in the introduction, the bioassays informed us about clear inter-galectin differences and dependence of inhibition on the conformational properties of the calix[n]arene scaffold as well as on the shape and valency of the glycoclusters. They raise the possibility of targeting galectins differently, cone-4Lac[4]Prop emerging as blocker of galectin-3 binding to colon cancer cells, flexible calix[6,8]arenes 6Lac[6]Met and 8Lac[8]Met for galectin-4 binding to pancreatic carcinoma cells, and alt-4Lac[4]Prop as inhibitor of galectins-1 and -4.

Experimental Section

General: Moisture-sensitive reactions were carried out under a nitrogen atmosphere. Dry solvents were prepared according to stan-

standard procedures and stored over molecular sieves. Melting points were determined in an electrothermal apparatus in capillaries sealed under nitrogen. ^1H and ^{13}C NMR spectra (300 and 75 MHz, respectively) were obtained on a Bruker AV300 spectrometer; partially deuterated solvents were used as internal standards; for ^1H NMR spectra recorded in D_2O at 90°C correction of chemical shifts was performed using the expression $\delta = 5.060 - 0.0122 \times T(^{\circ}\text{C}) + (2.11 \times 10^{-5}) \times T(^{\circ}\text{C})^2$.^[19] Mass spectra were recorded in ESI mode on a single quadrupole Micromass ZMD instrument (capillary voltage = 3 kV, cone voltage = 30–160 V, extractor voltage = 3 V, source block temperature = 80°C , desolvation temperature = 150°C , cone and desolvation gas (N_2) flow-rates = 1.6 and 8 L min^{-1} , respectively). TLC were performed on silica gel Merck 60 F_{254} , and flash chromatography using 32–63 μm , 60 Å Merck silica gel. *p*-*Tert*-butyl-*O*-alkylated calixarenes **1a**,^[20] **1b**,^[21] **1c**,^[22] **1d**,^[23] and **1e**,^[23] nitro derivatives **2a**,^[24] **2b**,^[22b] **2c**,^[22b] **2d**,^[24] **2e**,^[24] and 5,17-dinitro-25,26,27,28-tetramethoxycalix[4]arene,^[25] amino derivatives **3a**,^[8] **3b**,^[22b] **3c**,^[26] **3d**,^[24] and **3e**,^[24] tetragalactosyl derivatives **4a**,^[8] and *cone*-4Gal[4]Prop,^[8] digalactosyl *cone*-2Gal[4]Prop,^[8] and dilactosyl derivative *cone*-2Lac[4]Prop,^[8] were synthesized according to the literature procedures. 5,17-Diamino-25,26,27,28-tetramethoxycalix[4]arene, precursor of **6** and **7**, was obtained following the reduction procedure reported in the scheme and previously described^[24] and its spectroscopic and physical data are fully in agreement to those reported in literature.^[25]

Conjugation of glycosylisothiocyanate to aminocalixarenes: The aminocalixarene, the glycosylisothiocyanate (2 equiv for each amino group) and NEt_3 (2 equiv for each amino group) were dissolved in dry CH_2Cl_2 (10 mL for 0.1 mmol of calixarene), and the mixture was stirred at RT in nitrogen atmosphere. The reaction was stopped by evaporation of the solvent, and the crude purified by flash column chromatography or crystallization.

5,11,17,23-Tetrakis[(2,3,4,6-tetra-*O*-acetyl- β -D-galactopyranosyl)thioureido]-25,26,27,28-tetramethoxycalix[4]arene (4b**):** Reaction time: 24 h. The crude was purified by flash column chromatography on silica gel (eluent: hexane/AcOEt/ CH_3OH 6:4:1) and the pure product obtained as white solid in 67% yield. M.p. $177\text{--}179^\circ\text{C}$; ^1H NMR (300 MHz, $[\text{D}_6]\text{DMSO}$, 90°C): $\delta = 9.49$ (brs, 4H; ArNH), 7.61 (brs, 4H; ArNHCSNH), 7.08 (brs, 8H; Ar), 5.88 (t, $J = 9.6$ Hz, 4H; H1), 5.32–5.28 (m, 8H; H3, H4), 5.88 (t, $J = 9.3$ Hz, 4H; H2), 4.24 (t, $J = 6.3$ Hz, 4H; H5), 4.04 (d, $J = 6.3$ Hz, 8H; H6a,b), 3.52 (brs, 20H; ArCH₂Ar, OCH₃), 2.11, 2.03, 2.00, 1.94 ppm (4 s, 12H each; CH₃CO); ^{13}C NMR (75 MHz, $[\text{D}_6]\text{DMSO}$): $\delta = 181.1$ (CS), 170.0, 169.7, 169.6, 169.2 (CO), 154.8, 134.0, 133.1, 123.9 (Ar), 81.5, 71.1, 70.6, 68.1, 67.4, 61.1 (C1–C6), 59.9 (OCH₃), 36.2 30.5 (ArCH₂Ar), 20.4, 20.3, 20.2 ppm (OCCH₃); ESI-MS: m/z (%): 2120.9 (100) $[M+\text{Na}]^+$.

5,11,17,23-Tetrakis[(2,3,4,6-tetra-*O*-acetyl- β -D-galactopyranosyl)thioureido]-25,26,27,28-tetrapropoxycalix[4]arene-1,3-*alternate* (4c**):** Reaction time: 24 h. The crude was purified by flash column chromatography on silica gel (eluent: hexane/AcOEt/ CH_3OH 7:3:2) and the pure product obtained as white solid in 74% yield. M.p. $166\text{--}168^\circ\text{C}$; ^1H NMR (300 MHz, CDCl_3): $\delta = 8.12$ (s, 4H; ArNH), 6.94 (brs, 4H; ArNHCSNH), 6.91 and 6.90 (2 d, $J = 2.4$ Hz, 4H each; Ar), 5.84 (t, $J = 8.9$ Hz, 4H; H1), 5.45 (d, $J = 3.0$ Hz, 4H; H4), 5.19 (dd, $J = 10.2$, 3.0 Hz, 4H; H3), 5.11 (t, $J = 10.2$ Hz, 4H; H2), 4.16–4.07 (m, 12H; H5, H6a,b), 3.75–3.68 (m, 8H; OCH₂CH₂CH₃), 3.63, 3.61 (2 s, 4H each; ArCH₂Ar), 2.14, 2.06, 1.98 (3 s, 48H; OCCH₃), 1.85–1.70 (m, 8H; OCH₂CH₂CH₃), 0.95 ppm (t, $J = 7.4$ Hz, 12H; OCH₂CH₂CH₃); ^{13}C NMR (75 MHz, CDCl_3): $\delta = 182.6$ (CS), 170.8, 170.4, 169.9, 169.6 (CO), 155.5, 134.5, 129.4, 127.5, 127.2 (Ar), 83.6 (C1), 74.4 (OCH₂CH₂CH₃), 72.4, 70.9, 68.3, 67.1, 60.8 (C2–C6), 35.8 (ArCH₂Ar), 23.7 (OCH₂CH₂CH₃), 20.8, 20.7, 20.6, 20.5 (CH₃CO), 10.3 ppm

(OCH₂CH₂CH₃); ESI-MS: m/z (%): 1127.6 (100) $[M+2\text{Na}]^{2+}$, 2232.7 (20) $[M+\text{Na}]^+$.

5,11,17,23,29,35-Hexakis[(2,3,4,6-tetra-*O*-acetyl- β -D-galactopyranosyl)thioureido]-25,26,27,28,29,30-hexamethoxycalix[6]arene (4d**):** Reaction time: 48 h. The pure product was obtained by crystallization at 4°C from methanol in 57% yield. M.p. $180\text{--}182^\circ\text{C}$; ^1H NMR (300 MHz, CD_3OD): $\delta = 7.06$ (s, 12H; Ar), 5.94 (brs, 6H; H1), 5.35 (brs, 6H; H4), 5.26–5.21 (m, 12H; H2, H-3), 4.21–4.11 (m, 18H; H5, H6a,b), 3.98 (s, 12H; ArCH₂Ar), 3.32 (s, 18H; OCH₃), 1.97 ppm (m, 72H; CH₃CO); ^{13}C NMR (75 MHz, CDCl_3): $\delta = 181.7$ (s, CS), 171.2, 170.4, 169.9, 169.5 (s, CO), 155.5, 135.6, 135.1, 126.1, 124.9, (Ar), 83.1 (C1), 73.2, 72.7, 70.1, 67.9, 61.9 (C2–C6), 60.7 (OCH₃), 30.2 (ArCH₂Ar), 20.9, 20.7, 20.5, 20.3 ppm (CH₃CO); ESI-MS: m/z (%): 3170.0 (85) $[M+\text{Na}]^+$, 3170.0 (70) $[M+\text{Na}]^{2+}$, 1596.4 (100) $[M+2\text{Na}]^{2+}$.

5,11,17,23,29,35,41,47-Octakis[(2,3,4,6-tetra-*O*-acetyl- β -D-galactopyranosyl)thioureido]-49,50,51,52,53,54,55,56-octamethoxycalix[8]arene (4e**):** Reaction time: 48 h. The pure product was obtained by crystallization at 4°C from methanol in 60% yield. M.p. $188\text{--}190^\circ\text{C}$; ^1H NMR (300 MHz, CD_3OD): $\delta = 7.03$ (s, 16H; Ar), 5.89 (brs, 8H; H1), 5.44 (m, 8H; H4), 5.25–5.19 (m, 16H; H2, H3), 4.17–4.12 (m, 24H; H5, H6a,b), 4.06 (s, 16H; ArCH₂Ar), 3.56 (s, 24H; OCH₃), 1.99 ppm (m, 96H; CH₃CO); ^{13}C NMR (75 MHz, CD_3OD): $\delta = 181.8$ (CS), 170.8, 170.5, 169.8, 169.6 (CO), 155.2, 135.1, 131.6, 125.8 (Ar), 82.7 (C1), 73.5, 73.0, 70.5, 68.2, 61.6 (C2–C6), 60.9 (OCH₃), 29.8 (ArCH₂Ar), 20.8, 20.6, 20.4, 20.2 ppm (CH₃CO); ESI-MS: m/z (%): 2162.9 (80) $[M+2\text{Na}]^{2+}$.

5,17-Bis[(2,3,4,6-tetra-*O*-acetyl- β -D-galactopyranosyl)thioureido]-25,26,27,28-tetramethoxycalix[4]arene (6**):** Reaction time: 24 h. The crude was purified by flash column chromatography on silica gel (eluent: hexane/AcOEt/ CH_3OH 8:4:0.5) and the pure product obtained as white solid in 69% yield. M.p. $175\text{--}178^\circ\text{C}$; ^1H NMR (300 MHz, CD_3OD , 70°C): $\delta = 7.02$, 6.76 (2 brs, 10H; Ar), 5.93 (s, 2H; H1), 5.43 (s, 2H; H4), 5.26, 5.23 (dd, $J = 10.8$, 3.6 Hz, 2H; H3), 5.14 (t, $J = 10.8$ Hz, 2H; H2), 4.20–4.05 (brs, 6H; H5, H6a,b), 3.90–3.50 (brs, 20H; OCH₃, ArCH₂Ar), 2.09, 2.06, 2.00, 1.95 ppm (4 s, 6H each; CH₃CO); ^{13}C NMR (75 MHz, CD_3OD): $\delta = 183.4$ (CS), 172.5, 172.4, 172.2, 171.7 (CO), 158.2, 137.2, 136.8, 132.5, 130.3, 127.6, 126.4, 126.0, 124.3 (Ar), 84.5 (C1), 73.7, 73.0, 70.1, 69.2, 62.8 (C2–C6), 61.8, 61.5 (OCH₃), 37.0, 31.7 (t, ArCH₂Ar), 21.2, 21.0, 20.9, 20.8 ppm (CH₃CO); ESI-MS: m/z (%): 1311.8 (100) $[M+\text{Na}]^+$.

5,11,17,23-Tetrakis[(2,3,6-tri-*O*-acetyl-4-*O*-(2,3,4,6-tetra-*O*-acetyl- β -D-galactopyranosyl)-1- β -D-glucopyranosyl)thioureido]-25,26,27,28-tetrapropoxycalix[4]arene-*cone* (5a**):** Reaction time 24 h. The crude was purified by flash column chromatography (eluent (gradient): hexane/AcOEt/ CH_3OH 3.5:1.5:1–3:2:1) and the pure compound obtained as white solid in 90% yield. M.p. $172\text{--}173^\circ\text{C}$; ^1H NMR (300 MHz, CD_3CN , 70°C): $\delta = 8.08$ (s, 4H; ArNH), 6.63 (brs, 4H; ArNHCSNH), 6.47, 6.44 (2 d, $J = 2.4$ Hz, 4H each; Ar), 5.59 (brt, 4H; H1), 5.17 (brs, 4H; H4'), 5.10 (t, $J = 8.7$ Hz, 4H; H3), 4.89 (dd, $J = 10.2$, 3.0 Hz, 4H; H3'), 4.85–4.72 (m, 8H; H2', H2), 4.47 (d, $J = 7.8$ Hz, 4H; H1'), 4.40–4.20 (m, 8H; H6a, ArCH₂Ar), 4.05–3.80 (m, 24H; H4, H5, H6b, H5', H6'a,b), 3.76 (brt, 8H; OCH₂CH₂CH₃), 3.07 (d, $J = 13.2$ Hz, 4H; ArCH₂Ar), 2.15–1.70 (m, 92H; OCH₂CH₂CH₃, CH₃CO), 0.90 ppm (t, $J = 6.9$ Hz, 12H; OCH₂CH₂CH₃); ^{13}C NMR (CD_3CN , 75 MHz): $\delta = 183.1$ (CS), 171.3, 171.2, 170.4, 170.0 (CO), 155.1, 136.2, 131.0, 125.5 (Ar), 101.0 (C1'), 82.8 (C1), 76.7 (OCH₂CH₂CH₃), 77.6, 74.6, 73.1, 71.4, 71.1, 69.6, 67.8, 62.7, 61.7 (C2–C6, C2'–C6'), 30.9 (ArCH₂Ar), 23.7 (OCH₂CH₂CH₃), 20.8, 20.6, 20.4 (CH₃CO), 10.3 ppm (OCH₂CH₂CH₃); ESI-MS: m/z (%) 3385.0 (45) $[M+\text{Na}]^+$, 3385 (50) $[M+\text{Na}]^+$, 1703.7 (100) $[M+2\text{Na}]^{2+}$.

5,11,17,23-Tetrakis[(2,3,6-tri-O-acetyl-4-O-(2,3,4,6-tetra-O-acetyl- β -D-galactopyranosyl)-1- β -D-glucopyranosyl)thioureido]-25,26,27,28-tetramethoxycalix[4]arene (5b): Reaction time 24 h. The crude was purified by flash column chromatography (eluent: hexane/AcOEt/CH₃OH 3:2:1) and the pure compound obtained as white solid in 70% yield. M.p. 181–183 °C; ¹H NMR (300 MHz, CD₃OD, 60 °C): δ = 6.77 (brs, 8H; Ar), 5.86 (brd, 4H; H1), 5.35 (m, 8H; H4', H3), 5.07–4.96 (m, 12H; H3', H2', H2), 4.72 (d, J = 7.8 Hz, 4H; H1'), 4.45 (brd, 4H; H6a), 4.22–4.05 (m, 20H; H5, H6b, H5', H6'a,b), 3.98–3.62 (m, 28H; H4, ArCH₂Ar, OCH₃), 2.13, 2.04, 1.92 ppm (3 s, 84H; CH₃CO); ¹³C NMR (75 MHz, CD₃OD, 60 °C): δ = 182.9 (CS), 172.5, 172.1, 172.0, 171.7, 171.5, 171.2 (CO), 157.6, 137.0, 134.5, 125.9 (Ar), 101.8 (C1'), 83.9 (C1), 77.3, 75.7, 74.2, 72.5, 72.2, 71.8, 70.6, 68.6, 63.7, 62.2, 61.5 (C2-C6, C2'-C6', OCH₃), 31.5 (ArCH₂Ar), 21.2, 21.0, 20.8, 20.5 ppm (CH₃CO); ESI-MS: m/z (%) 3272.8 (30) [M+Na]⁺, 1648.4 (100) [M+2Na]²⁺.

5,11,17,23-Tetrakis[(2,3,6-tri-O-acetyl-4-O-(2,3,4,6-tetra-O-acetyl- β -D-galactopyranosyl)-1- β -D-glucopyranosyl)thioureido]-25,26,27,28-tetrapropoxycalix[4]arene-1,3-alternate (5c): Reaction time 24 h at 65 °C in a sealed tube. The crude was purified by flash column chromatography (eluent: hexane/AcOEt/CH₃OH 3:2:1) and the pure compound obtained as white solid in 79% yield. M.p. 168–170 °C; ¹H NMR (300 MHz, CDCl₃): δ = 7.95 (s, 4H; ArNH), 6.84 (brs, 12H; Ar, ArNHCSNH), 5.78 (t, J = 8.7 Hz, 4H; H1), 5.40–5.25 (m, 8H; H4', H3), 5.07 (dd, J = 10.2, 7.8 Hz, 4H; H2'), 4.91 (dd, J = 10.2, 3.0 Hz, 4H; H3'), 4.85 (t, J = 8.7 Hz, 4H; H2), 4.46–4.40 (brs, 4H; H6a), 4.43 (d, J = 7.8 Hz, 4H; H1'), 4.25–3.96 (m, 12H; H5, H6b, H6'a), 3.92–3.75 (m, 12H; H6'b, H5', H4), 3.66 (t, J = 7.2 Hz, 8H; OCH₂CH₂CH₃), 3.54 (s, 8H; ArCH₂Ar), 2.12, 2.03, 2.02, 2.01, 1.93 (5 s, 84H; CH₃CO), 1.78–1.62 (m, 8H; OCH₂CH₂CH₃), 0.91 ppm (t, J = 7.2 Hz, 12H; OCH₂CH₂CH₃); ¹³C NMR (CDCl₃, 75 MHz): δ = 182.5 (CS), 170.7, 170.3, 170.0, 169.9, 169.2, 168.9 (CO), 155.3, 134.4, 129.3, 126.7 (Ar), 100.7 (C1'), 82.9 (C1), 75.8, 74.5, 72.5, 70.9, 70.6, 68.9, 66.5, 61.9, 60.8 (C2-C6, C2'-C6', OCH₂CH₂CH₃), 38.1 (ArCH₂Ar), 23.6 (OCH₂CH₂CH₃), 20.9, 20.7, 20.6, 20.55, 20.4 (CH₃CO), 10.2 ppm (OCH₂CH₂CH₃); ESI-MS: m/z (%) 3385.7 (50) [M+Na]⁺, 1704.4 (100) [M+2Na]²⁺.

5,11,17,23,29,35-Hexakis[(2,3,6-tri-O-acetyl-4-O-(2,3,4,6-tetra-O-acetyl- β -D-galactopyranosyl)-1- β -D-glucopyranosyl)thioureido]-25,26,27,28,29,30-hexamethoxycalix[6]arene (5d): Reaction time 24 h. The pure product was obtained as a white solid in 80% yield by trituration with Et₂O and subsequent crystallization from CH₂Cl₂/Et₂O. M.p. 201–205 °C; ¹H NMR (300 MHz, [D₆]DMSO, 90 °C): δ = 9.50 (s, 6H; ArNH), 7.74 (brd, 6H; ArNHCSNH), 7.17 (brs, 12H; Ar), 5.78 (t, J = 9.0 Hz, 6H; H1), 5.25–5.10 (m, 18H; H4', H3, H3'), 4.92–4.80 (m, 12H; H2, H2'), 4.76 (d, J = 7.8 Hz, 6H; H1'), 4.32 (d, J = 11.7 Hz, 6H; H6a), 4.21 (m, 6H; H5'), 4.15–3.97 (m, 24H; H5, H6b, H6'a,b), 3.90–3.75 (m, 18H; H4, ArCH₂Ar), 3.24 (brs, 18H; OCH₃), 2.09, 2.05, 2.02, 2.00, 1.96, 1.90 ppm (6 s, 126H; CH₃CO); ¹³C NMR (75 MHz, [D₆]DMSO): δ = 181.5 (CS), 170.2, 169.9, 169.6, 169.5, 169.3, 169.0 (CO), 152.8, 133.9, 123.8 (Ar), 99.7 (C1'), 80.9 (C-1), 76.0, 73.2, 72.9, 70.6, 70.4, 69.7, 68.8, 67.0, 62.3, 60.9 (C2-C6, C2'-C6'), 60.0 (OCH₃), 29.7 (ArCH₂Ar), 20.7, 20.4, 20.3, 20.2 ppm (CH₃CO); ESI-MS: m/z (%) 3385.7 (20) [M+Na]⁺, 1704.4 (40) [M+2Na]²⁺.

5,11,17,23,29,35,41,47-Octakis[(2,3,6-tri-O-acetyl-4-O-(2,3,4,6-tetra-O-acetyl- β -D-galactopyranosyl)-1- β -D-glucopyranosyl)thioureido]-49,50,51,52,53,54,55,56-octamethoxycalix[8]arene (5e): Reaction time: 48 h. The crude was purified by flash column chromatography (eluent: hexane/AcOEt/CH₃OH 2.5:2.5:1) and the pure compound obtained as white solid in 68% yield. M.p. 190–192 °C; ¹H NMR (300 MHz, [D₆]DMSO, 90 °C): δ = 9.51 (s, 8H; ArNH), 7.76

(brs, 8H; ArNHCSNH), 7.13 (s, Ar), 5.76 (t, J = 8.7 Hz, 8H; H1), 5.30–5.11 (m, 24H; H4', H3, H3'), 4.95–4.82 (m, 16H; H2, H2'), 4.76 (d, J = 7.8 Hz, 8H; H1'), 4.31 (brd, 8H; H6a), 4.19 (brt, 8H; H5'), 4.12–3.95 (m, 24H; H5, H6b, H6'a,b), 4.00–3.75 (overlapped broad signals, 16H; ArCH₂Ar, H4), 3.41 (brs, OCH₃), 2.10, 2.03, 2.02, 2.00, 1.94 ppm (5 s, 168H; CH₃CO). ¹³C NMR (75 MHz, [D₆]DMSO): δ = 181.3 (CS), 170.0, 169.6, 169.3, 169.0, 168.8 (CO), 152.7, 133.9, 133.3, 123.7, 123.6, 123.5 (Ar), 99.4 (C1'), 80.6 (C1), 75.8, 73.0, 72.7, 70.3, 70.2, 69.4, 68.5, 66.8, 62.0, 60.6, 60.1 (C2-C6, C2'-C6', OCH₃), 29.3 (ArCH₂Ar), 20.2, 20.1, 20.0, 19.9, 19.8 ppm (CH₃CO); ESI-MS: m/z (%): 3274.40 (20) [M+2Na]²⁺, 2190.1 (35) [M+3Na]³⁺.

5,17-Bis[(2,3,6-tri-O-acetyl-4-O-(2,3,4,6-tetra-O-acetyl- β -D-galactopyranosyl)-1- β -D-glucopyranosyl)thioureido]-25,26,27,28-tetramethoxycalix[4]arene (7): Reaction time: 24 h. The crude was purified by flash column chromatography (eluent: hexane/AcOEt/CH₃OH 3:2:1) and the pure compound obtained as white solid in 81% yield. M.p. 190–192 °C; ¹H NMR (300 MHz, CD₃CN, 80 °C): δ = 8.11 (brs, 2H; ArNH), 7.00–6.50 (2brs, 12H; Ar, ArNHCSNH), 5.68 (brt, J = 7.1 Hz, 2H; H1), 5.19 (d, J = 2.7 Hz, 2H; H4'), 5.12 (t, J = 9 Hz, 2H; H-3), 4.90 (dd, J = 10.4, 3.3 Hz, 2H; H3'), 4.90–4.80 (m, 2H; H2'), 4.74 (t, J = 9.0 Hz, 2H; H2), 4.47 (d, J = 7.8 Hz, 2H; H1'), 4.26 (d, J = 12.0 Hz, 2H; H6a), 4.02–3.81 (m, 10H; H5, H6b, H5', H6'a,b), 3.78–3.30 (m and brs, 22H; H4, ArCH₂Ar, OCH₃), 1.95, 1.91, 1.88, 1.87, 1.77 ppm (s, 42H; CH₃CO); ¹³C NMR (75 MHz, CD₃CN): δ = 182.2 (CS), 171.1, 170.8, 170.4, 170.3, 170.0 (CO), 158.1, 136.5, 135.3, 133.5, 131.0, 128.9, 126.2, 125.2, 124.9, 123.0, 122.3 (Ar), 101.1 (C1'), 82.9 (C1), 76.7, 74.7, 73.2, 71.4, 71.2, 69.6, 67.8, 62.7, 61.7 (C2-C6, C2'-C6'), 60.6 (OCH₃), 37.4, 31.0 (ArCH₂Ar), 20.8, 20.6, 20.4 ppm (CH₃CO); ESI-MS: m/z (%) 1887.9 (100) [M+Na]⁺.

Deprotection from acetyl groups: The protected glycosylthioureido calixarene was suspended in dry CH₃OH, and the pH was adjusted to 8–9 by addition of a solution of CH₃ONa in CH₃OH. The reaction was stirred at RT for 45 min and quenched by addition of Amberlite IR120 (H⁺) resin until neutral pH. The resin was filtered off, and the solvent was removed under reduced pressure to obtain the pure deprotected glycolcalixarene.

5,11,17,23-Tetra[(β -D-galactopyranosyl)thioureido]-25,26,27,28-tetramethoxycalix[4]arene (4Gal[4]Met): Yield: 98%. M.p. 152–154 °C (dec); ¹H NMR (300 MHz, D₂O): δ = 7.17, 7.03 (2 s, 4H each; Ar), 5.46 (brs, 4H; H1), 3.95 (brs, 4H; H4), 3.77–3.62 (overlapped m, 20H; H2, H3, H5, H6a,b), 3.75 (s, 8H, ArCH₂Ar), 3.45 ppm (s, 12H; OCH₃); ¹³C NMR (75 MHz, D₂O/CD₃OD 4:1, v/v): δ = 183.6 (s, CS), 155.8, 136.7, 129.9, 128.5 (Ar), 86.1 (C-1), 77.7, 74.7, 70.7, 69.9, 62.1, (C2-C-6), 59.2 (OCH₃), 36.8 ppm (ArCH₂Ar); ESI-MS: m/z (%) 735.8 (100) [M+2Na]²⁺, 1447.8 (20) [M+Na]⁺.

5,11,17,23-Tetra[(β -D-galactopyranosyl)thioureido]-25,26,27,28-tetrapropoxycalix[4]arene-1,3-alternate (alt-4Gal[4]Prop): Yield: 97%. M.p. 110–112 °C (dec); ¹H NMR (300 MHz, CD₃OD): δ = 7.16, 7.11 (2 s, 4H each; Ar), 5.44 (brs, 4H; H1), 3.94 (d, J = 3.0 Hz, 4H; H4), 3.81 (s, 8H, ArCH₂Ar), 3.81–3.57 (overlapped signals, 28H; OCH₂CH₂CH₃, H2, H3, H5, H6a,b), 1.80–1.60 (m, 8H; OCH₂CH₂CH₃), 0.89 ppm (t, J = 7.2 Hz, 12H; OCH₂CH₂CH₃); ¹³C NMR (75 MHz, CD₃OD): δ = 184.7 (CS), 156.1, 136.2, 133.9, 129.5, 129.2 (Ar), 86.7 (C1), 78.5 (OCH₂CH₂CH₃), 76.1, 75.8, 71.8, 70.8, 62.9 (C2-C6), 38.2 (ArCH₂Ar), 24.7 (OCH₂CH₂CH₃), 10.8 ppm (OCH₂CH₂CH₃). ESI-MS: m/z (%) 1559.5 (100) [M+Na]⁺.

5,11,17,23,29,35-Hexakis[(β -D-galactopyranosyl)thioureido]-25,26,27,28,29,30-hexamethoxycalix[6]arene (6Gal[6]Met): Yield: 90%. M.p. 98–100 °C (dec.); ¹H NMR (300 MHz, D₂O, 90 °C): δ = 6.91 (s, 12H; Ar), 5.29 (brs, 6H; H1), 3.92 (s, 12H; ArCH₂Ar), 3.98–3.56 (overlapped brs, 36H; H2-H6a,b), 3.08 ppm (s, 18H; OCH₃);

^{13}C NMR (75 MHz, $[\text{D}_6]\text{DMSO}$): $\delta = 182.3$ (CS), 153.1, 134.8, 134.3, 126.0 (Ar), 83.5 (C1), 78.6, 77.9, 73.1, 70.2, 61.1 (C2-C6), 60.5 (OCH_3), 30.9 ppm (ArCH_2Ar); ESI-MS: m/z (%): 2160.0 (50) $[\text{M}+\text{Na}]^+$, 1091.7 (100) $[\text{M}+2\text{Na}]^{2+}$.

5,11,17,23,29,35,41,47-Octakis[(β -D-galactopyranosyl)thioureido]-49,50,51,52,53,54,55,56-octamethoxycalix[8]arene (8Gal[8]-Met): Yield: 98%. M.p. 100–102 °C (dec.); ^1H NMR (300 MHz, D_2O , 90 °C): $\delta = 6.86$ (brs, 16H; Ar), 5.23 (brs, 8H; H1), 3.84 (brs, 16H; ArCH_2Ar), 3.78, 3.54 (2brs, 48H; H2-H6a,b), 3.25 ppm (brs, 24H; OCH_3); ^{13}C NMR (75 MHz, $[\text{D}_6]\text{DMSO}$): $\delta = 182.7$ (CS), 153.4, 134.5, 126.2 (Ar), 84.7 (C1), 76.9, 74.6, 70.4, 68.8, 61.2 (C2-C6), 58.5 (OCH_3), 30.1 ppm (ArCH_2Ar); ESI-MS: m/z (%): 1447.2 (100) $[\text{M}+2\text{Na}]^{2+}$.

5,17-Bis[(β -D-galactopyranosyl)thioureido]-25,26,27,28-tetramethoxycalix[4]arene (2Gal[4]Met): By deprotection of **6**. Yield: 93%. M.p. 184–186 °C (dec.); ^1H NMR (300 MHz, CD_3OD): $\delta = 7.32$ –7.22 (brs, 2H; ArNH), 7.20–7.00, 7.00–6.80, 6.60–6.35 (brs, 12H; Ar, ArNHCSNH), 5.60–5.30 (brs, 2H; H1), 4.37 (d, $J = 12.7$ Hz, 3.4H; ArCH_2Ar cone), 4.20–4.00, 4.00–3.55 (brs, 23.2H; H2, H3, H4, H5, H6a,b, OCH_3 , ArCH_2Ar 1,3-alternate), 3.21 ppm (d, $J = 12.7$ Hz, 3.4H; ArCH_2Ar); ^{13}C NMR (75 MHz, CD_3OD): $\delta = 183.3$, 182.9, 182.7 (CS), 160.4, 157.2, 156.8, 156.6, 137.0, 135.7, 134.5, 131.7, 130.0, 126.1, 125.5, 125.1, 124.0, 122.8 (Ar), 86.1 (C1), 78.1, 75.7, 71.7, 70.5, 62.5 (C2-C6), 61.5, 60.6, 60.3, 60.0 (OCH_3), 36.6, 31.4 ppm (ArCH_2Ar); ESI-MS: m/z (%): 975.2 (100) $[\text{M}+\text{Na}]^+$.

5,11,17,23-Tetrakis[(β -D-galactopyranosyl)-1- β -D-glucopyranosyl]thioureido]-25,26,27,28-tetrapropoxycalix[4]arene-cone (cone-4Lac[4]Prop): Yield: 80%. M.p. 135–137 °C (dec.); ^1H NMR (300 MHz, D_2O , 90 °C): $\delta = 6.72$ (brs, 8H; ArH), 5.40 (brs, 4H; H1), 4.40 (brs, 4H; H1'), 4.23 (brs, 4H, ArCH_2Ar), 3.95–3.35 (overlapped brs, 56H; H2-H6a,b, H2'-H6'a,b, $\text{OCH}_2\text{CH}_2\text{CH}_3$), 3.10 (brs, 4H; ArCH_2Ar), 1.77 (brs, 8H; $\text{OCH}_2\text{CH}_2\text{CH}_3$), 0.85 ppm (brs, 12H; $\text{OCH}_2\text{CH}_2\text{CH}_3$); ^{13}C NMR (75 MHz, $[\text{D}_6]\text{DMSO}$): $\delta = 182.4$ (CS), 154.1, 134.8, 133.8, 124.4 (Ar), 104.1 (C1'), 83.9 (C1), 76.8 ($\text{OCH}_2\text{CH}_2\text{CH}_3$), 80.2, 76.6, 76.0, 73.6, 72.6, 71.2, 68.8, 61.1, 60.6 (C2-C6, C2'-C6'), 30.9 (ArCH_2Ar), 23.3 ($\text{OCH}_2\text{CH}_2\text{CH}_3$), 10.7 ppm ($\text{OCH}_2\text{CH}_2\text{CH}_3$); ESI-MS: m/z (%): 2207.8 (65) $[\text{M}+\text{Na}]^+$, 1115.5 (100) $[\text{M}+2\text{Na}]^{2+}$.

5,11,17,23-Tetrakis[(β -D-galactopyranosyl)-1- β -D-glucopyranosyl]thioureido]-25,26,27,28-tetramethoxycalix[4]arene (4Lac[4]Met): Yield: 90%. M.p. 137–139 °C (dec.); ^1H NMR (300 MHz, D_2O): $\delta = 7.27$, 7.10 (brs, 4H each; Ar), 5.47 (brd, 4H; H1), 4.42 (brd, 4H; H1'), 3.92–3.37 (overlapped signals, 60H; H2-H6a,b, H2'-H6'a,b, OCH_3), 3.73 ppm (s, 8H, ArCH_2Ar); ^{13}C NMR (75 MHz, D_2O): $\delta = 183.5$ (CS), 156.2, 137.6, 129.3, 128.5 (Ar), 104.4 (C1'), 85.4 (d, C1), 79.8, 77.6, 76.7, 76.4, 73.9, 73.0, 72.3, 69.9, 62.4, 61.3 (C2-C6, C2'-C6'), 60.0 (OCH_3), 36.9 ppm (ArCH_2Ar); ESI-MS: m/z (%): 2096.7 (20) $[\text{M}+\text{Na}]^+$, 1059.7 (100) $[\text{M}+2\text{Na}]^{2+}$.

5,11,17,23-Tetrakis[(β -D-galactopyranosyl)-1- β -D-glucopyranosyl]thioureido]-25,26,27,28-tetrapropoxycalix[4]arene-1,3-alternate (alt-4Lac[4]Prop): Yield: 82%. M.p. 160–162 °C (dec.); ^1H NMR (300 MHz, D_2O): $\delta = 7.38$, 7.19 (2brs, 2H each; Ar), 5.49 (brd, 4H; H1), 4.50 (d, 4H; H1'), 4.09–3.57 (overlapped m, 48H; H2-H6a,b, H2'-H6'a,b), 3.72 (s, 8H, ArCH_2Ar), 3.45 (brt, 8H; $\text{OCH}_2\text{CH}_2\text{CH}_3$), 1.62 (brs, 8H; $\text{OCH}_2\text{CH}_2\text{CH}_3$), 0.91 ppm (brt, $J = 7.2$ Hz, 12H; $\text{OCH}_2\text{CH}_2\text{CH}_3$); ^{13}C NMR (75 MHz, D_2O): $\delta = 183.6$ (CS), 155.6, 137.4, 136.8, 134.0, 130.2, 129.3 (Ar), 104.6 (C1'), 85.4 (C1), 80.1, 77.7, 76.9, 76.2, 74.1, 73.1, 72.4, 70.0, 62.5, 61.5 (C2-C6, C2'-C6', $\text{OCH}_2\text{CH}_2\text{CH}_3$), 38.0 (ArCH_2Ar), 24.4 ($\text{OCH}_2\text{CH}_2\text{CH}_3$), 11.0 ppm ($\text{OCH}_2\text{CH}_2\text{CH}_3$); ESI-MS: m/z (%): 2207.6 (40) $[\text{M}+\text{Na}]^+$, 1115.3 (80) $[\text{M}+2\text{Na}]^{2+}$.

5,11,17,23,29,35-Hexakis[(β -D-galactopyranosyl)-1- β -D-glucopyranosyl]thioureido]-25,26,27,28,29,30-hexamethoxycalix[6]arene

(6Lac[6]Met): This compound was obtained pure by column chromatography on Sephadex G25 (eluent: H_2O). Yield: 82%. M.p. 150–152 °C (dec.); ^1H NMR (300 MHz, D_2O + 5% $[\text{D}_6]\text{DMSO}$, 90 °C): $\delta = 6.80$ (brs, 12H; Ar), 5.18 (brd, 6H; H1), 4.18 (brd, 6H; H1'), 3.80–2.60 ppm (overlapped brm, 90H; H2-H6a,b, H2'-H6'a,b, OCH_3), 3.71 ppm (brs, 12H, ArCH_2Ar); ^{13}C NMR (75 MHz, D_2O + 5% $[\text{D}_6]\text{DMSO}$, 90 °C): $\delta = 183.1$ (CS), 156.8, 135.3, 133.5, 126.6 (Ar), 103.5 (C1'), 84.4 (C1), 79.1, 74.7, 73.3, 72.6, 71.6, 69.2, 61.4, 61.1, 58.6 (C2-C6, C2'-C6', OCH_3), 30.8 ppm (ArCH_2Ar); ESI-MS: m/z (%): 1578.4 (100) $[\text{M}+2\text{Na}]^{2+}$, 1059.8 (100) $[\text{M}+3\text{Na}]^{3+}$.

5,11,17,23,29,35,41,47-Octakis[(β -D-galactopyranosyl)-1- β -D-glucopyranosyl]thioureido]-49,50,51,52,53,54,55,56-octamethoxycalix[8]arene (8Lac[8]Met): This compound was obtained pure after crystallization from CH_3OH . Yield: 74%. M.p. 142–143 °C (dec.); ^1H NMR (300 MHz, D_2O , 90 °C): $\delta = 6.81$ (brs, 16H; Ar), 5.24 (brs, 8H; H1), 4.27 (brd, 8H; H1'), 3.77–3.03 (overlapped brs, 120H; H2-H6a,b, H2'-H6'a,b, OCH_3), 3.75 ppm (brs, 16H, ArCH_2Ar); ^{13}C NMR (75 MHz, D_2O , 90 °C): $\delta = 184.1$ (CS), 154.1, 134.7, 132.5, 127.9 (Ar), 102.2 (C1'), 82.7 (C1), 79.5, 77.7, 73.1, 71.3, 69.0, 61.2, 60.8, 60.6, 57.8, (C2-C6, C2'-C6', OCH_3), 30.1 ppm (ArCH_2Ar); ESI-MS: m/z (%): 2095.3 (70) $[\text{M}+2\text{Na}]^{2+}$.

5,17-Bis[(β -D-galactopyranosyl)-1- β -D-glucopyranosyl]thioureido]-25,26,27,28-tetramethoxycalix[4]arene (2Lac[4]Met): By deprotection of **7**, the pure product was obtained by column chromatography on Sephadex G25 (eluent: $\text{H}_2\text{O}/\text{CH}_3\text{OH}$ 95:5, v/v). Yield: 85%. M.p. 190–192 °C (dec.); ^1H NMR (300 MHz, CD_3OD , 65 °C): $\delta = 7.05$, 6.82, 6.60–6.40 (3brs, 10H; ArH), 5.50 (brs, 4H; H1), 4.38 (d, $J = 7.5$ Hz, 4H; H1'), 3.90–3.40 ppm (overlapped m, 32H; H2-H6a,b and H2'-H6'a,b', ArCH_2Ar , OCH_3); ^{13}C NMR (75 MHz, CD_3OD): $\delta = 183.3$ (CS), 159.9, 159.2, 157.1, 156.7, 137.3, 135.8, 134.7, 133.6, 131.9, 130.0, 126.3, 125.1, 124.2, 122.8 (Ar), 105.1 (C1'), 85.4 (C1), 80.6, 77.9, 77.3, 77.1, 74.7, 73.6, 72.5, 70.3, 62.6, 61.9 (C2-C6, C2'-C6'), 61.5, 61.2, 60.5 (OCH_3), 36.7, 31.5 ppm (ArCH_2Ar); ESI-MS: m/z (%): 1297.5 (100) $[\text{M}+\text{Na}]^+$.

Molecular modeling: Because of the large number of atoms, the analysis of the conformation of 8Lac[8]Met was undertaken using a force field in the framework of classical molecular mechanics (MMFF in the Spartan suite).^[27] For calixarenes, as for other macrocycles such as cyclodextrins, a computational approach based on a classical description of molecules is widely accepted.^[28] Calculations were carried out on a Pentium IV PC at 2.5 MHz.

Lectins: The mistletoe lectin was purified from extracts of dried leaves using affinity chromatography on lactosylated Sepharose 4B, obtained by divinyl sulfone activation, as the crucial step, human galectins-1 and -3 were obtained by recombinant production as described and similarly purified.^[13,29] The starting material for cloning of human galectin-4-specific cDNA was total RNA from the human acute myelogenous leukemia line KG-1 (American Type Culture Collection, Rockville, MD, USA) using first the sense primer 5'-GTACGCATATGCGCTATGCCCCGACC-3' with an internal NdeI restriction site (underlined) and the antisense primer 5'-GCTAGGTCGACTTAGATCTGGACATAGG-3' with an internal Sall restriction site (underlined). The cDNA of human galectin-4s N-domain was obtained by using the sense primer 5'-CATATGCGCTATGCCCCG-CACCG-3' with an internal NdeI restriction site (underlined) and the antisense primer 5'-GTCCGACTTAGATCTGGACATAGGACAAGGTG-3' with an internal Sall restriction site (underlined). To delete the sequence coding for the linker peptide of the tandem-repeat-type lectin we first amplified the cDNAs for the two domains separately and took advantage of the two HindIII restriction sites to create a new joining hinge of the shortened cDNA. In detail, we used the

following primer pairs: the sense primer 5'-CATATGGCCTATG-TCCCCGCACCG-3' with an internal NdeI restriction site (underlined) and the antisense primer 5'-AAGCTTGAAGTTGATTGATTGAAGTTG-CAG-3' with an internal HindIII restriction site (underlined) for the N-domain and the sense primer 5'-AAGCTTGTGCCATATTCGG-GAGG-3' with an internal HindIII restriction site (underlined) and the antisense primer 5'-GTCCGACTTAGATCTGGACATAGG-3' with an internal Sall restriction site (underlined) for the C-domain. The cDNAs were then propagated in the pET-Blue-1 Acceptor vector (Novagen, Bad Soden, Germany), digestion with the restriction enzymes and gel extraction led to vector-released cDNAs (972 bp for the full-length protein, 453 bp for the N-domain, 852 bp for protein version without the linker peptide). They were ligated into pET12a (full-length protein, N-domain; Novagen, Darmstadt, Germany) or pET24a (human galectin-4 without linker; Novagen, Darmstadt, Germany). The inserted HindIII restriction site at the boundary between the N- and C-domains encoding for Lys and Leu finally needed to be reversed to the wild-type codons, at these positions encoding for Ile and Pro. The pET24a plasmid containing the cDNA encoding for human galectin-4 without the linker peptide was therefore employed as template in a modified Quik-Change® site-directed mutagenesis procedure (Stratagene Europe, Amsterdam, The Netherlands).^[30] To do this, a suitable primer set (sense primer 5'-GCAACTCAATCAATCACTTCATCCCTGTGCCA-TATTCGGGAGG-3' (nucleotide exchanges underlined) and the antisense primer 5'-CCTCCGAAATATGGCACAGGGATGAAGTTGATT-GATTGAAGTTGC-3' (nucleotide exchanges underlined)) was designed with melting temperatures > 78 °C. The extension reaction was performed in two steps. Briefly, two 50 µL reaction mixtures were prepared in separate tubes containing 20 pmol either of the sense or the antisense primer, 200 ng template plasmid and 1 U *PfuTurbo*® DNA polymerase (Stratagene Europe, Amsterdam, The Netherlands). After an initial preheating step at 95 °C for 30 s, three cycles (denaturation at 95 °C for 30 s, annealing at 55 °C for 1 min, extension at 68 °C for 8 min) were run. To complete the primer-directed sequence extension 25 µL of each tube were transferred to one tube and 1 U *PfuTurbo*® DNA polymerase was added. Subsequently, thermal cycling which consisted of preheating at 94 °C for 30 s and 18 cycles (denaturation at 94 °C for 30 s, annealing at 55 °C for 1 min, extension at 68 °C for 5 min) was carried out. After incubation with DpnI (10 U) at 37 °C for 2 h to digest the methylated parental DNA template, 5 µL of the reaction mixture were used to transform XL-1-Blue electrocompetent cells. Plasmids were isolated from kanamycin-resistant colonies grown on LB agar plates and ascertained for correct reversion of the artificial HindIII restriction site to the wild-type sequence by commercial DNA sequencing. Recombinant production was accomplished in the pET-12a or 24a/*E. coli* strain BL21(DE3)pLysS system with TB medium (Roth, Karlsruhe, Germany) at 30 °C with a final IPTG concentration of 100 µM, reaching optimal yields for full-length human galectin-4 (17–21 mg L⁻¹), for the N-domain (3.3–5.8 mg L⁻¹), and for the lectin without the linker peptide (13.3–30.3 mg L⁻¹). Quality controls by one- and two-dimensional gel electrophoreses, mass spectrometry, gel filtration, and haemagglutination to ascertain homogeneity, quaternary structure, and activity as well as biotinylation of the lectins under activity-preserving conditions followed by product analysis to quantify label incorporation and activity were performed as described.^[4a, 13, 29, 31]

Inhibition assays: Adsorption of the glycoprotein to the surface of microtiter plates proceeded from 50 µL per well at 4 °C overnight from phosphate-buffered saline, residual protein-binding sites were saturated with 100 µL of a 1% solution of carbohydrate-free bovine serum albumin at 37 °C for 1 h. Lectin binding in the ab-

sence and presence of glycocluster was carried out for 1 h at 37 °C, routinely running controls with lactose and galactose in parallel, and the extent of bound lectin was determined spectrophotometrically at 490 nm with streptavidin-peroxidase conjugate (0.5 µg mL⁻¹; Sigma, Munich, Germany) as indicator and o-phenylenediamine (1 mg mL⁻¹)/H₂O₂ (1 µL mL⁻¹) as chromogenic substrates as described.^[13, 17a] Cell culture of the human B-lymphoblastoid line Croco II, the colon adenocarcinoma line SW480, and the human pancreatic carcinoma line Capan-1 with reconstituted expression of the tumor suppressor p16^{INK4a} (kindly provided by K. M. Detjen, Berlin, Germany) was performed using routine procedures, and lectin binding to cells using biotinylated proteins was determined by quantitative fluorescence detection in a FACScan instrument (Becton-Dickinson, Heidelberg, Germany) by using streptavidin/R-phycoerythrin (1:40; Sigma) as indicator.^[13, 32] In cases of solubility problems stock solutions of the glycoclusters were prepared in dimethyl sulfoxide and then diluted in buffer. Final concentrations of aprotic solvent was up to 4.4% at 2.5 mM inhibitor concentration in solid-phase assays and up to 6.8% in cell assays. Parallel controls with the identical solvent concentration in the absence of glycocluster ascertained the lack of a significant solvent effect on lectin activity, as reported previously.^[33]

Acknowledgements

This work was partially supported by an EC Marie Curie Research Training Network grant (contract no. MCRN-CT-2005-19561), the Ministero dell'Università e della Ricerca (MUR) PRIN (project no. 2006034123), the research initiative "LMUexcellent" and the Verein zur Förderung des biologisch-technologischen Fortschritts in der Medizin e.V. (Heidelberg, Germany). We are indebted to the Centro Interdipartimentale Misure of the University of Parma for use of NMR facilities and Drs. B. Friday and S. Namirha for inspiring discussions.

Keywords: calixarene · glycoconjugates · lectin · metastasis · multivalency · tumor

- [1] a) N. Sharon, H. Lis in *Glycosciences: Status and Perspectives* (Eds.: H.-J. Gabius, S. Gabius, Chapman & Hall, London, 1997, pp. 133–162; b) G. Reuter, H.-J. Gabius, *Cell. Mol. Life Sci.* 1999, 55, 368–422; c) J. B. Lowe, J. D. Marth, *Annu. Rev. Biochem.* 2003, 72, 643–691; d) H.-J. Gabius, *Crit. Rev. Immunol.* 2006, 26, 43–80.
- [2] a) H.-J. Gabius, H.-C. Siebert, S. André, J. Jiménez-Barbero, H. Rüdiger, *ChemBioChem* 2004, 5, 740–764; b) A. Villalobo, A. Nogales-González, H.-J. Gabius, *Trends Glycosci. Glycotechnol.* 2006, 18, 1–37.
- [3] a) K.-i. Kasai, J. Hirabayashi, *J. Biochem.* 1996, 119, 1–8; b) H.-J. Gabius, *Eur. J. Biochem.* 1997, 243, 543–576; c) K. Kayser, D. Hoefl, P. Hufnagl, J. Caselitz, Y. Zick, S. André, H. Kaltner, H.-J. Gabius, *Histol. Histopathol.* 2003, 18, 771–779; d) N. Nagy, H. Legendre, O. Engels, S. André, H. Kaltner, K. Wasano, Y. Zick, J.-C. Pector, C. Decaestecker, H.-J. Gabius, I. Salmon, R. Kiss, *Cancer* 2003, 97, 1849–1858; e) S. Langbein, J. Brade, J. K. Badawi, M. Hatzinger, H. Kaltner, M. Lensch, K. Specht, S. André, U. Brinck, P. Alken, H.-J. Gabius, *Histopathology* 2007, 51, 681–690.
- [4] a) S. André, P. C. O. Ortega, M. A. Perez, R. Roy, H.-J. Gabius, *Glycobiology* 1999, 9, 1253–1261; b) A. M. Wu, J. H. Wu, J.-H. Liu, T. Singh, S. André, H. Kaltner, H.-J. Gabius, *Biochimie* 2004, 86, 317–326; c) S. André, T. Kožár, R. Schuberth, C. Unverzagt, S. Kojima, H.-J. Gabius, *Biochemistry* 2007, 46, 6984–6995; d) A. M. Wu, T. Singh, J.-H. Liu, M. Krzeminski, R. Russwurm, H.-C. Siebert, A. M. J. J. Bonvin, S. André, H.-J. Gabius, *Glycobiology* 2007, 17, 165–184.
- [5] a) D. A. Fulton, J. F. Stoddart, *Bioconjugate Chem.* 2001, 12, 655–672; b) C. Ortiz Mellet, J. Defaye, J. M. García Fernández, *Chem. Eur. J.* 2002,

- 8, 1982–1990; c) A. Casnati, F. Sansone, R. Ungaro, *Acc. Chem. Res.* **2003**, *36*, 246–254; d) O. Renaudet, P. Dumy, *Org. Lett.* **2003**, *5*, 243–246; e) O. Hayashida, I. Hamachi, *J. Org. Chem.* **2004**, *69*, 3509–3516; f) L. Baldini, A. Casnati, F. Sansone, R. Ungaro, *Chem. Soc. Rev.* **2007**, *36*, 254–266; g) S. K. Pandey, X. Zheng, J. Morgan, J. R. Missert, T.-H. Liu, M. Shibata, D. A. Bellnier, A. R. Oseroff, B. W. Henderson, T. J. Dougherty, R. K. Pandey, *Mol. Pharm.* **2007**, *4*, 448–464.
- [6] a) J. M. García Fernández, C. Ortiz Mellet, *Adv. Carbohydr. Chem. Biochem.* **2000**, *55*, 35–135; b) A. Casnati, F. Sansone, R. Ungaro, *Adv. Supramol. Chem.* **2003**, *9*, 165–218.
- [7] In order to facilitate the reader in identifying the structure of the calixarene ligands, we introduced in the text the running nomenclature *conf-m[S]nAlk*. For each compound, the conformation *conf*, when it is well defined, the number *m* and the type of saccharide *S*, the size *[n]* of the macrocycle, between square brackets as usually used in the name calix[n]arene, and the alkyl chain *Alk* corresponding to the substituent at the phenolic oxygen of the macrocycle are indicated.
- [8] F. Sansone, E. Chierici, A. Casnati, R. Ungaro, *Org. Biomol. Chem.* **2003**, *1*, 1802–1809.
- [9] C. Jaime, J. de Mendoza, P. Prados, P. M. Nieto, C. Sanchez, *J. Org. Chem.* **1991**, *56*, 3372–3376.
- [10] a) S. Kanamathareddy, C. D. Gutsche, *J. Am. Chem. Soc.* **1993**, *115*, 6572–6579; b) S. Kanamathareddy, C. D. Gutsche, *J. Org. Chem.* **1994**, *59*, 3871–3879.
- [11] a) R. T. Lee, Y. C. Lee in *Glycosciences: Status and Perspectives* (Eds.: H.-J. Gabius, S. Gabius), Chapman & Hall, London, **1997**, 55–77; b) T. K. Dam, C. F. Brewer, *Chem. Rev.* **2002**, *102*, 387–429.
- [12] a) R. T. Lee, H.-J. Gabius, Y. C. Lee, *J. Biol. Chem.* **1992**, *267*, 23722–23727; b) O. E. Galanina, H. Kaltner, L. S. Khraltsova, N. V. Bovin, H.-J. Gabius, *J. Mol. Recognit.* **1997**, *10*, 139–147; c) S. Bharadwaj, H. Kaltner, E. Y. Korchagina, N. V. Bovin, H.-J. Gabius, A. Surovia, *Biochim. Biophys. Acta Gen. Subj.* **1999**, *1472*, 191–196; d) M. Jiménez, S. André, H.-C. Siebert, H.-J. Gabius, D. Solís, *Glycobiology* **2006**, *16*, 926–937.
- [13] S. André, H. Kaltner, T. Furuiki, S.-I. Nishimura, H.-J. Gabius, *Bioconjugate Chem.* **2004**, *15*, 87–98.
- [14] a) S. André, B. Liu, H.-J. Gabius, R. Roy, *Org. Biomol. Chem.* **2003**, *1*, 3909–3916; b) N. Ahmad, H.-J. Gabius, S. André, H. Kaltner, S. Sabesan, R. Roy, B. Liu, F. Macaluso, C. F. Brewer, *J. Biol. Chem.* **2004**, *279*, 10841–10847.
- [15] T. K. Dam, H.-J. Gabius, S. André, H. Kaltner, M. Lensch, C. F. Brewer, *Biochemistry* **2005**, *44*, 12564–12571.
- [16] a) H. Ideo, A. Seko, T. Ohkura, K. L. Matta, K. Yamashita, *Glycobiology* **2002**, *12*, 199–208; b) A. M. Wu, J. H. Wu, M.-C. Tsai, J.-H. Liu, S. André, K. Wasano, H. Kaltner, H.-J. Gabius, *Biochem. J.* **2002**, *367*, 653–664; c) D. Delacour, V. Gouyer, J.-P. Zanetta, H. Drobecq, E. Leteurte, G. Grard, D. Moreau-Hannedouche, E. Maes, A. Pons, S. André, A. Le Bivic, H.-J. Gabius, A. Manninen, K. Simons, G. Huet, *J. Cell Biol.* **2005**, *169*, 491–501; d) H. Ideo, A. Seko, K. Yamashita, *J. Biol. Chem.* **2005**, *280*, 4730–4737; e) H. Ideo, A. Seko, K. Yamashita, *J. Biol. Chem.* **2007**, *282*, 21081–21089.
- [17] a) N. Kondoh, T. Wakatsuki, A. Ryo, A. Hada, T. Aihara, S. Horiuchi, N. Goseki, O. Matsubara, K. Takenaka, M. Shichita, K. Tanaka, M. Shuda, M. Yamamoto, *Cancer Res.* **1999**, *59*, 4990–4996; b) Y. Hippo, M. Yashiro, M. Ishii, H. Taniguchi, S. Tsutsumi, K. Hirakawa, T. Kodama, H. Aburatani, *Cancer Res.* **2001**, *61*, 889–895; c) M. E. Huflejt, H. Leffler, *Glycoconjugate J.* **2003**, *20*, 247–255; d) C. Sakakura, K. Hasegawa, K. Miyagawa, S. Yazumi, H. Yamagishi, T. Okanoue, T. Chiba, A. Hagiwara, *Clin. Cancer Res.* **2005**, *11*, 6479–6488; e) V. A. Heinzelmann-Schwarz, M. Gardiner-Garden, S. M. Henshall, J. P. Scurry, R. A. Scolyer, A. N. Smith, A. Bali, A. van den Berg, S. Baron-Hay, C. Scott, D. Fink, N. F. Hacker, R. L. Sutherland, P. M. O'Brien, *Br. J. Cancer* **2006**, *94*, 904–913.
- [18] a) S. André, Z. Pei, H.-C. Siebert, O. Ramström, H.-J. Gabius, *Bioorg. Med. Chem.* **2006**, *14*, 6314–6326; b) S. Fort, H.-S. Kim, O. Hindsgaul, *J. Org. Chem.* **2006**, *71*, 7146–7154; c) S. André, C. E. P. Maljaars, K. M. Halkes, H.-J. Gabius, J. P. Kamerling, *Bioorg. Med. Chem. Lett.* **2007**, *17*, 793–798; d) I. Cumpstey, E. Salomonsson, A. Sundin, H. Leffler, U. J. Nilsson, *ChemBioChem* **2007**, *8*, 1389–1398.
- [19] H. E. Gottlieb, V. Kotlyar, A. Nudelman, *J. Org. Chem.* **1997**, *62*, 7512–7515.
- [20] E. Kelderman, L. Derhaeg, G. J. T. Heesink, W. Verboom, J. F. J. Engbersen, *Angew. Chem.* **1992**, *104*, 1107–1110; *Angew. Chem. Int. Ed. Engl.* **1992**, *31*, 1075–1077.
- [21] C. D. Gutsche, B. Dhawan, J. A. Levine, K. H. No, L. J. Bauer, *Tetrahedron* **1983**, *39*, 409–426.
- [22] a) K. Iwamoto, K. Araki, S. Shinkai, *J. Org. Chem.* **1991**, *56*, 4955–4962; b) F. Sansone, M. Dudič, G. Donofrio, C. Rivetti, L. Baldini, A. Casnati, S. Cellai, R. Ungaro, *J. Am. Chem. Soc.* **2006**, *128*, 14528–14536.
- [23] S.-K. Chang, I. Cho, *J. Chem. Soc. Perkin Trans. 1* **1986**, 211–214.
- [24] M. Dudič, A. Colombo, F. Sansone, A. Casnati, G. Donofrio, R. Ungaro, *Tetrahedron* **2004**, *60*, 11613–11618.
- [25] P. Timmerman, J.-L. Weidmann, K. A. Jolliffe, L. J. Prins, D. N. Reinhoudt, S. Shinkai, L. Frish, Y. Cohen, *J. Chem. Soc. Perkin Trans. 2* **2000**, 2077–2089.
- [26] G. Mislin, E. Graf, M. W. Hosseini, *Tetrahedron Lett.* **1996**, *37*, 4503–4506.
- [27] SPARTAN 04, Release 1.01. 2004. Wavefunction, Inc., 18401 von Karman Avenue, Suite 370, Irvine, CA 92612, USA; <http://www.wavefun.com>.
- [28] F. C. J. M. van Veggel in *Calixarenes in Action* (Eds.: L. Mandolini, R. Ungaro), Imperial College Press, London, **2000**, pp. 11–36.
- [29] a) H.-J. Gabius, *Anal. Biochem.* **1990**, *189*, 91–94; b) M. Jiménez, J. L. Sáiz, S. André, H.-J. Gabius, D. Solís, *Glycobiology* **2005**, *15*, 1386–1395.
- [30] W. Wang, B. A. Malcolm, *BioTechniques* **1999**, *26*, 680–682.
- [31] T. Purkrábková, K. Smetana, Jr., B. Dvořánková, Z. Holíková, C. Böck, M. Lensch, S. André, R. Pytlík, F.-T. Liu, J. Klíma, K. Smetana, J. Motlík, H.-J. Gabius, *Biol. Cell* **2003**, *95*, 535–545.
- [32] S. André, H. Sanchez-Ruderisch, H. Nakagawa, M. Buchholz, J. Kopitz, P. Forberich, W. Kemmer, C. Böck, K. Deguchi, K. M. Detjen, B. Wiedemann, M. von Knebel Doeberitz, T. M. Gress, S.-I. Nishimura, S. Rosewicz, H.-J. Gabius, *FEBS J.* **2007**, *274*, 3233–3256.
- [33] H.-C. Siebert, S. André, J. L. Asensio, F. J. Cañada, X. Dong, J. F. Espinosa, M. Frank, M. Gilleron, H. Kaltner, T. Kožár, N. V. Bovin, C.-W. von der Lieth, J. F. G. Vliegthart, J. Jiménez-Barbero, H.-J. Gabius, *ChemBioChem* **2000**, *1*, 181–195.

Received: January 18, 2008

Published online on May 28, 2008